Morpho-sedimentary dynamics associated to dam removal. The Pierre Glissotte dam (central France)

Louis Gilet, Frédéric Gob, Clément Virmoux, E Gautier, Nathalie Thommeret, Nicolas Jacob-Rousseau

Morpho-sedimentary dynamics associated to dam removal. The Pierre Glissotte dam (central France).

Louis Gilet*[a], Frédéric Gob[a], Clément Virmoux[a], Emmanuèle Gautier[a], Nathalie Thommeret[b], Nicolas Jacob-Rousseau[c]

[a] Université Panthéon-Sorbonne (Paris 1), Laboratoire de Géographie Physique, CNRS UMR8591, 1 Place Aristide Briand, FR 92195 Meudon cedex, France

[b] Laboratoire Geomatique et Foncier, CNAM-ESGT, 1 Boulevard Pythagore, 72000 Le Mans, France

[c] Laboratoire Archéorient, UMR 5133 CNRS - Université Lumière (Lyon 2), Maison de l'Orient et de la Méditerranée, 7 Rue Raulin, 69365 Lyon cedex 07, France.

*Corresponding author. E-mail address: Louis.GILET@lgp.cnrs.fr

Keywords: River restoration; Bedload continuity; Morpho-sedimentary adjustments; Hydromorphological trajectory; Yonne River.

1. Introduction

Dam removal has greatly increased since the 1990s, particularly in the USA where 1,700 removals were recorded in February 2020 in the American Rivers database (www.americanrivers.org). Different goals or needs motivate this type of operation: safety and economic issues when there is a risk of dam failure or when the dam is approaching its engineered life expectancy and incurring increasing maintenance costs; landscape and eco-geomorphic problems when the purpose of the removal is river restoration (Bellmore et al., 2017; Major et al., 2017). In the latter case, the objective of establishing "natural components and regenerative processes" (Hart et al., 2002) relies to a great extent on restoring fish passages and sediment continuity. The reactivation of hydro-sedimentary dynamics is often expected to re-shape the river at different spatial scales, modifying channel morphology, the fluvial landscape and fauna and flora habitats. Several dozen operations have been studied and published in connection with one or more hydromorphological aspects (e.g. Egan and Pizutto, 2000; Stanley and Doyle, 2003; Major et al, 2012; Randle et al., 2015; Ibisate et al., 2016; Magilligan et al., 2016; Gilet et al., 2018). Based on numerous case studies, a series of reviews have already gathered and compared findings in the literature on the geomorphic effects of dam removal (Skalak and Pizutto, 2005; Sawaske and Freyberg, 2012; Grant and Lewis, 2015; Bellmore *et al.*, 2017; Foley et al., 2017a, b; Major et al., 2017).

Although some common trends in river adjustments have emerged from these studies, the reviews also emphasize the many interacting factors that influence the river response at local scale and may prevent the accurate prediction of the impacts of dam removal: the time that has elapsed since the dam was first built; the distance from the dam of a given reach; the size of the dam; the volume of sediment and the composition of the reservoir fill; the location of the dam in the river network; the hydromorphological context (the geology and morphology, flow and sediment regime, morphological features, etc.), the anthropogenic context and history of the river (Foley et al., 2017a; Major et al., 2017; Poeppl et al., 2017). Despite possible similarities, it is hard to predict differences in the way the many hydro-physical conditions will interact with each other from one site to another (Bellmore et al., 2019). Uncertainty in how the river will respond also arises when unexpected discoveries are made during the removal operation such as anthropogenic structures (Wilcox *et*

al., 2014; Magilligan et al., 2016) or different substrate materials (Harris and Evans, 2014; Gartner et al., 2015) that control incision or lateral erosion. Ultimately, exactly where and when adjustments will occur in a given river reach cannot be foreseen. Indeed, changes in the dynamics and rates of the river response in space and over time make predicting the river trajectory complex (Major et al., 2017).

All these sources of uncertainty - differences in the chain of interactions and feedback between sites, unexpected discoveries, spatial and temporal variations in the response of a river at the same site, but also changes in the hydromorphological conditions in the period between when the dam was constructed and its removal - make it difficult to predict exactly how the river will respond, and to guarantee beforehand that it will return to its pre-dam hydromorphological and ecological state (Foley et al., 2017a; Bellmore et al., 2019). However, rivers' responses to dam removal help to inform the discussion around restoration and rehabilitation paradigms (Dufour and Piégay, 2009). Only a few studies have sought to interpret the post-removal conditions (forms and processes) in the hydromorphological trajectory: do they correspond to a pre-dam equilibrium? Do the conditions implemented under the dam's influence still prevail? Has a completely new hydromorphological equilibrium emerged? The meaning of restoring sediment dynamics should also be questioned: when fill sediments are significantly eroded and the reestablishment of sediment continuity is successful, does it lead to the restoration of the hydromorphological functioning of the river? How much time does the restoration or the achievement of a new functioning require? This last question and the frequently changing patterns in river adjustment to dam removal contribute to the need for long term studies to fully grasp the effects of dam removal at different time scales (Foley et al., 2017a). Until now, even when the long-term response was being assessed (Evans, 2007; Skalak et al., 2011; Peck and Kasper, 2013), most of the studies were short-term (1-2 years) (Bellmore et al., 2017).

Our paper reports on a four-year study of river readjustment after the removal of the 90-year-old and 7.3 m high Pierre Glissotte dam, located on the Yonne river. 1This gravel bed stream running through a medium-mountain range (Morvan massif) was deeply modified from the 16th century on by log driving, mills and damming. At the start of the 2010s, the reservoir was almost completely filled, mainly with fine sediments, stopping bedload particles at the entrance of the impoundment. The removal of the dam took place in two steps, one in July-August 2015 and the other in October 2017. The hydromorphological monitoring carried out during and after the sequenced removal of the Pierre Glissotte dam was accompanied by a study of current bedload transport dynamics of the Yonne River at two neighboring sites not directly affected by the

dam removal. The four-year monitoring project thus offered a good opportunity to: (i) examine the modes and response processes of a river whose bedload dynamics have been characterized at other sites around the structure; (ii) measure the hydromorphological adjustments, the patterns of change in morphodynamics (rates, timing, duration) and in driving mechanisms, and the spatial and temporal variations of these processes in the impoundment and in the downstream reach over a period of four years; (iii) examine the implications of restoring sediment continuity for the general hydromorphological functioning of the river around the former dam.

2. The upper Yonne river and the Pierre Glissotte hydroelectric complex

The Morvan massif is a Hercynian medium-elevation mountain range located in the southeastern part of the Seine catchment in central France, where the maximum altitude is 902 m (Fig. 1). The substratum is mainly granitic and gneissic rocks, and the climate is temperate oceanic with pluviometry influenced by the orography. Mean annual precipitation in the region is 900 mm. Combined with the impermeability of the substratum, this has led to the formation of a channel network with high drainage density. The landcover of the hillslopes in the upper Yonne catchment, where the Pierre Glissotte complex is located, is mainly meadows and forests (Fig. 2).

The engineering history of the upper Yonne river is old. Between the middle of the 16th century and the early 20th century, the river and its headwater tributaries were used for log driving. The significant geomorphological effects of log driving on the upper Yonne river were studied and characterized by Poux et al. (2011) and Jacob-Rousseau and Gob (2020). To give an example, management of the river for the log driving industry resulted in the bed degradation of the head water streams and in the aggradation of the upper Yonne river in its middle reach. The sediment stored in the Yonne river has not yet been removed.

The hydromorphological trajectory around the Pierre Glissotte dam period is far from linear. The Pierre Glissotte dam (supplementary material, Fig. S1A) was built between 1923 and 1927, after log driving was abandoned. Originally the 7.3 m high dam was built to provide electricity for nearby rubber factories. Hydroelectric production stopped, and the dam was then opened for 30 years (1955-1985) because the first hydroelectrical plant burned down. The dam started to function again in 1985, but in 2002 a storm stopped

the sluice gate functioning. As a result, in 2015, the Pierre Glissotte reservoir was almost completely filled with sediment (42 600 m^3, Gilet et al., 2018) and the dam acted as an obstacle to biological (there was no efficient fishway) and sediment continuity. The reservoir fill was mainly fine sediment composed of sand and silt. For the upper half of the reservoir fill, we were able to estimate that layers of sand (D_{50} = 153 µm) represented 40% of the deposit. The other materials corresponded to a mixture of silt ($14 \leq D_{50} \leq 21$ µm) and organic matter, the proportion of which increased near the dam (Gilet et al., 2018). Most of the pebbles and cobbles, the bedload of the Yonne river, were deposited in the tail of the reservoir (the tail coarse deposit formed between 1985 and 2015 has been estimated at 2,300 m^3). At the Pierre Glissotte dam, the mean discharge of the Yonne river is 2.1 m^3/s.

Another dam, the "Moulin Blondelot dam" is located 1,200 m upstream from the Pierre Glissotte dam (Fig. 2, and supplementary material, Fig. S1B), where the mean discharge of the Yonne River is 1.9 m3/s. This 3.49 m high dam creates only a small impoundment (700 m^3) and a mobile gate is automatically opened gradually during a flood event. A maximum discharge of 2.3 m^3/s is diverted from this dam to the Moulin Blondelot hydroelectric plant, located 820 m downstream. The tail race of the plant conducts the diverted discharge back to the Yonne river at the entrance of the Pierre Glissotte reservoir (Fig. 2). The maximum diversion capacity of the bypass canal, 2.3 m^3/s, mainly affects the small floods flowing into the bypassed reach. In addition, the bedload sediments flow easily through the Moulin Blondelot dam. These conditions and the steep bed slope of the Yonne river in the bypassed reach (1.5 % < s < 3.5 %) contribute to the active bedload transport in the section of the river leading to the Pierre Glissotte reservoir (Gilet et al., 2018; Gilet et al., 2020). Allowing sediment continuity through the Pierre Glissotte dam was consequently all the more necessary.

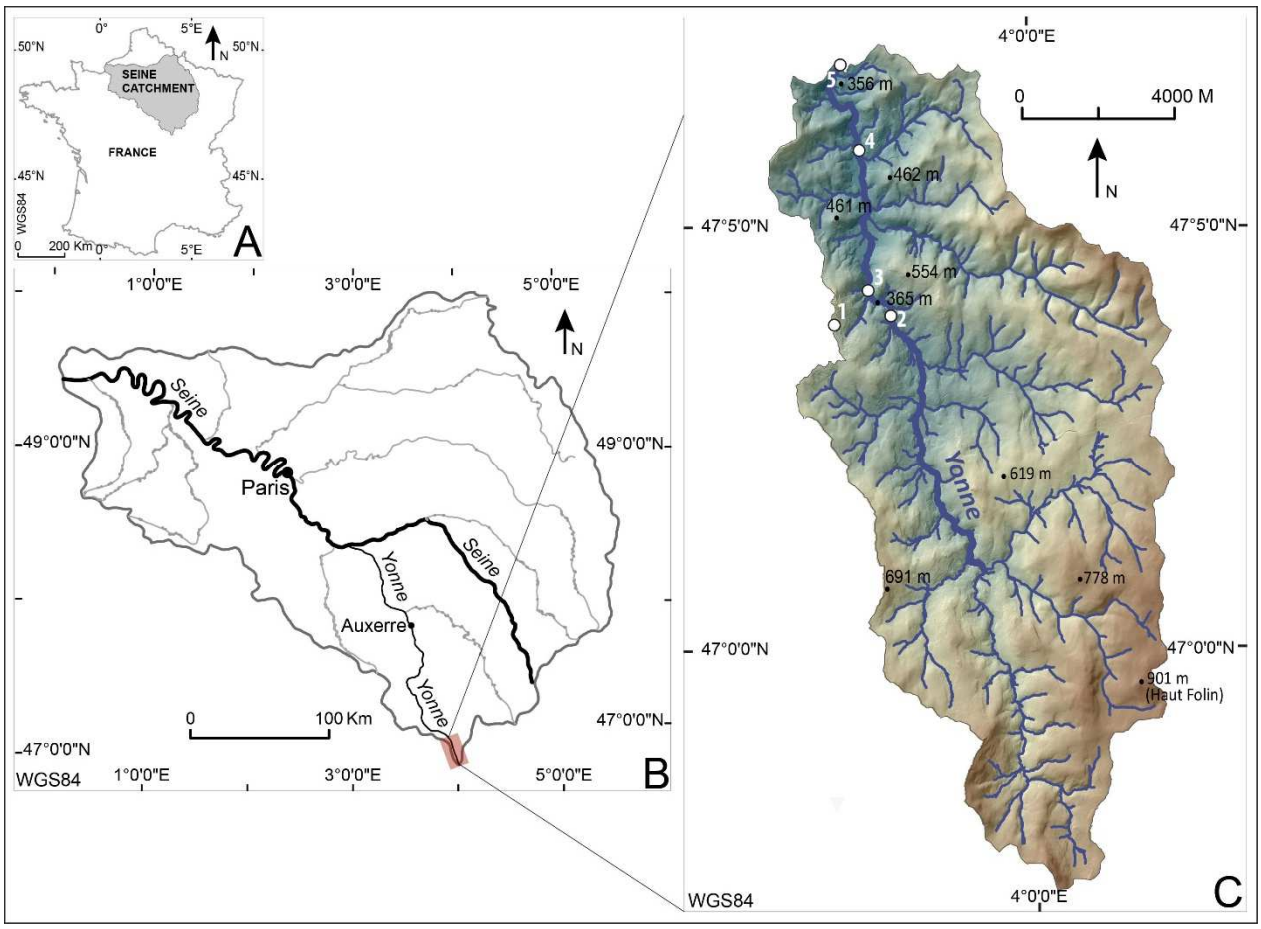

Fig. 1 Upper Yonne catchment and location of the Pierre Glissotte dam. Map C: 1. Château-Chinon city; 2. Moulin Blondelot dam; 3. Pierre Glissotte dam; 4. Corancy hydrometric station; 5. Tail of the Pannecière reservoir.

3. The removal project

The removal project was implemented by the private owner of the Pierre Glissotte complex (the Pierre Glissotte Hydroelectric Company) and the Seine Normandie Water Agency. Discussions began following the owner's need to modernize the Pierre Glissotte power plant to comply with the Water and Aquatic Environments Act (2006), i.e. restoring biological and sediment continuity. The managers of the water agency seized the opportunity to propose a project that would allow the uppermost part of the Yonne catchment (78 km^2) to be reconnected with another 32.5 km^2 of its catchment, between the Pierre Glissotte dam and the Pannecière reservoir located 5.5 km downstream (Fig. 2). The project proposed by the owner and the water agency was based on three main elements: (i) the removal of the Pierre Glissotte dam in two steps separated by a two-year period; (ii) the replacement of the fish pass at the Moulin Blondelot dam; (iii) the abandonment of the Moulin Blondelot hydroelectric power plant and the modernization of the Pierre

Glissotte hydroelectric power plant (Fig. 2). The latter would be provided with a new longer penstock extending the diversion canal that reached the Moulin Blondelot hydroelectric plant (Fig. 2). The new penstock started to function and bypass the reservoir reach in March 2016, with a maximum diversion capacity corresponding to that of the upstream diversion canal (2.3 m^3/s).

The emptying and water level drawdown of the Pierre Glissotte reservoir started on July 20, 2015. The emptying was operated using the butterfly valve and the old penstock that usually provided the Pierre Glissotte power plant with water. During the emptying, this penstock (soon to be replaced) was disconnected from the power plant and water was released in the river just downstream of the dam. The top three meters of the dam were removed between August 11 and August 17. The second stage of the removal took place between October 13 and October 17, 2017. The remaining 4 meters of the dam were removed but only from the right third of the valley width, so as to protect the renovated power plant located downstream of the dam, near the left hillslope. The river was thus partly channelized at the dam site and just upstream as large boulders were also placed on the left bank along 50 m to protect the water pipe (new penstock) that supplies the new turbines (supplementary material, Fig. S2).

4. Methods

Several tools and methods were used over the four-year monitoring period to assess the hydromorphological effects of the removal of the Pierre Glissotte dam. The flow regime was monitored with pressure probes. Bedload dynamics were investigated by individual tracing of coarse particles. Other methods were used to detect and quantify changes in the river's geometry and planforms: topographic surveys (total station), aerial photographs (drone) combined with SFM photogrammetry. Measurements of grain-size distribution (Wolman) in the riverbed completed the morpho-sedimentary characterization of the river's response. A complete overview of the workflow and methodology developed on the Yonne river is presented in Figure 2 and Tables 1 and 2. As shown in Table 2, the different methods were rarely implemented together and at all study sites during the same fieldwork campaign. Methodological strategy (e.g. one prime site / control sites) and practical necessities (logistics, practicability) are the reasons for this. The prime study site itself, Pierre Glissotte (R), is divided into three sub-reaches that were equipped and monitored differently: the former impoundment (Ri) and its immediate upstream (Ru) and downstream (Rd) reaches.

159 **4.1 Hydro-sedimentary monitoring**

160

161 To understand the consequences of the removal of the Pierre Glissotte dam on bedload transport, the
162 movement of particles was monitored individually using radio frequency identification (RFID) technology.
163 Tracking sediment mobility using RFID has become widespread in the last decade (Liébault et al., 2012;
164 Bradley and Tucker, 2012; Chapuis et al., 2014; Houbrechts et al., 2015, Dépret et al., 2017). We used
165 passive integrated transponders (PIT tag, Passive Integrated Transponder) from Texas Instruments and two
166 detection systems: one configured by the company *CIPAM* and the other by *Technologie Aquartis senc*. The
167 transponders we used are glass bulb type PIT tags, operating at low frequency (134.2 kHz), 23 mm or 32 mm
168 long and 3-4 mm thick. At each monitoring site, PIT tags were inserted into particles randomly taken from
169 the bed according to the pebble count method developed by Wolman (1954). The objective was to have
170 tagged particles (tracers) representative of the alluvium present in the bed. At the Pierre Glissotte study site
171 (R), the reservoir fill was occupied by fine particles. Tracers were therefore collected in the immediate
172 upstream reach, where the D_{50} of the riverbed equates 108 mm (Gilet et al., 2018, supplementary material,
173 Fig. S3). On average, tracers remained smaller than the particles in the riverbed (Table 1, and supplementary
174 material, Fig. S3) because of technical constraints (tracers not equipped on site).

175

176 In addition to the site of the former Pierre Glissotte dam reservoir (R), bedload transport was also monitored
177 at two control sites, upstream (U) and downstream (D), that were not influenced by the dismantling of the
178 structure (Fig. 2). These sites were also selected to represent the diversity of existing hydrological situations
179 in the study area (Table 1). Both were positioned outside the hydrological influence of the dams, upstream
180 and downstream of the study area (U is located 0.6 km upstream of the Moulin Blondelot dam and D is
181 located 1.3 km downstream of the Pierre Glissotte dam). The study of river reaches not affected by the
182 dismantling operation was expected to help inform our understanding of the specific functioning of a typical
183 transient site after the removal of a dam.

184

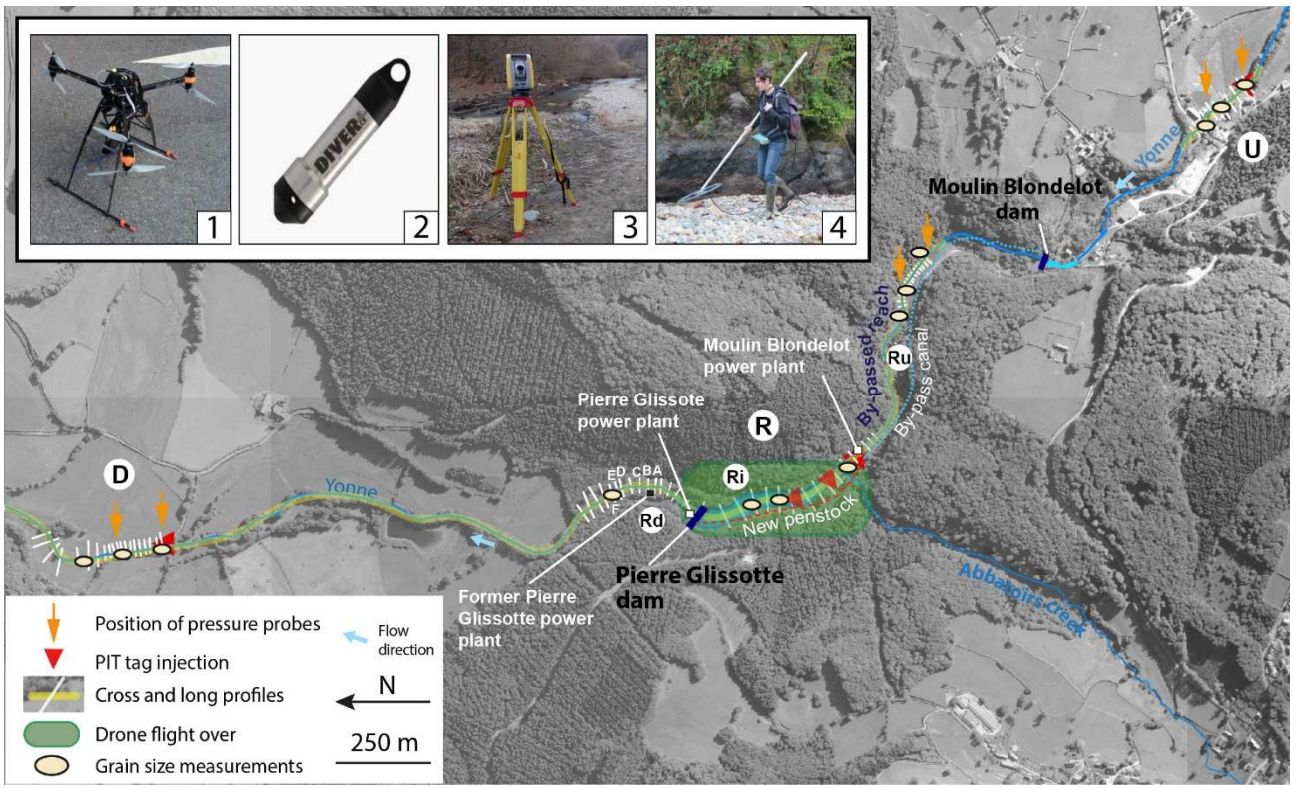

Fig. 2 Location of the study sites and overview of the methods and technologies. 1. Hexacopter drone; 2. Diver pressure probe (water level); 3. Total station Trimble S6; 4. PIT tag detection antenna. In Rd sub-reach, A, B, C, D, E, F correspond to the cross-sections of Figure 8.

Table 1. Location and characteristics of the study sites.

Site	Location with respect to the PG dam	Hydrological Regime	Slope (m/m)	Bankfull width (m)	Specific stream power for Qbf[a] (W/m^2)	D_{50} river bed (mm)	D_{50} tracers (mm)
U	Upstream	Not influenced	0.0073	9.5	45.2	74	59
D	Downstream	Not influenced	0.0085	11.7	67.7	83.5	63.5
Ri- Pierre Glissotte	Impoundment	Moderately Influenced[b]	Evolving	Evolving	Evolving	Evolving	52 (1st injection) 69 (2nd injection)
Ru-Pierre Glissotte	Immediately upstream the reservoir	Influenced[c]	0.015	10.5	77.1	104	No tracers
Rd-Pierre Glissotte	Immediately downstream the reservoir	Moderately influenced[d]	0.013	11.5	64.3	73.5	52 (1st injection) 69 (2nd injection)

[a] Qbf: Bankfull discharge

[b] No influence on the Pierre Glissotte site was observed between July 2015 and March 2016 (the time needed to extend the diversion canal from the former Moulin Blondelot power plant to the Pierre Glissotte plant). After, the reservoir reach was bypassed up to 2.3 m^3/s (a minimum discharge of 300 l/s must be left in the by-passed reach).

[c]The reach is bypassed up to 2.3 m3/s, with a minimum discharge required of 300 l/s (derivation of the discharge starts at the Moulin Blondelot dam).

[d]The first 95 m of the reach are by passed up to 2.3 m3/s for the functioning of the Pierre Glissotte plant (except for the July 2015-March 2016 interval, without discharge diversion).

Sites U and D were each equipped with 75 tracers: the first 50 were injected in October 2014 and the remaining 25 in October 2015. Site R in the former Pierre Glissotte reservoir (Ri) was equipped with 200 tracers in July 2015, just before the start of the reservoir emptying. At this time, the riverbed was composed of sandy and silty sediments of the reservoir filling (Gilet et al., 2018). The second series of 172 tracers were injected in July 2017, a few months before the second step of the removal (October 2017). At that time, a gravel riverbed had formed again ($41 \leq D_{50} \leq 61$). At each site and at each injection, the tracers were placed along several cross sections to avoid future detection "conflicts" (i.e. difficulties for the RFID reader to identify tracers that are very close). 10 "RFID cross sections" were used on U and D, 24 on Ri study site. A minimum distance of 2 m was left between each cross section and a distance of at least 1.20 m was left between each tracer along the same cross section. Subsequently, a flexible tape measure was unrolled along the bank to measure the distances travelled by the marked particles.

The distance travelled by the tracers was recorded five times at U and D, and 11 times at R between their injection and July 2019 (Table 2). RFID surveys were more numerous at Pierre Glissotte (R) as the system was transient. Moreover, conditions were more often favorable for detection surveys (low water depth) than on the U and D sites. The sites are also equipped with water pressure sensors (Diver ©Schlumberger) that record the water level at 15-minute intervals (Fig. 2). The water levels were transformed into discharge using stage-discharge relationships built from our own discharge measurements made with an electro-magnetic current-meter and extrapolations from data recorded at the Corancy hydrometric station (using a formula to adapt the calculated discharge to the size of the basin, Bravard and Petit, 1997). The Corancy hydrometric station is located only a few kilometers downstream from the study sites (from 4.5 to 1 km) (Fig. 1C). It drains the first 106 km² of the Yonne catchment and is not influenced by the Pierre Glissotte hydroelectric complex.

4.2 Morpho-sedimentary characterization of the Yonne riverbed

4.2.1 Topographic surveys

The morphology of study site was characterized using a Trimble S6 total station. At sites U and D, the longitudinal profile and cross-sectional geometry were measured from a series of cross-sections (n: 13 on U, n: 20 on D) to allow characterization of the channel geometry (Fig. 2). Several topographic survey campaigns including longitudinal and cross-sectional profiles to assess the morphological changes following the removal stages, were conducted in the former impoundment (Ri), and in its immediate upstream (Ru) and downstream (Rd) reaches (Table 2). The cross-sections were carried out on a different stretch of the river length depending on the area to be surveyed (upstream, reservoir, downstream) but always targeting intervals between cross-sections of 1.5 times the bankfull width. 13 cross-sections were carried out on Ri and 15 on Rd, and two series of 3 and 13 cross-sections were surveyed on Ru (the interval left between the two series is due to the impracticability of the fieldwork). A mean distance of 0.92 cm was left between each point of a cross-section within the channel. On the sections where only the long profile was surveyed, one point was measured on average every 1.5 m. In addition, a historic long-profile of the Yonne River (water surface) was available. It was surveyed in 1933, only a few years after the dam was completed in 1927. A study of the longitudinal changes in the Yonne River after 1933 and the methodological precision of the comparison with the current long profile are detailed in Gilet et al. (2018).

Table 2. Overview of the fieldwork campaigns and methods used in the former Pierre Glissotte impoundment (Ri), its immediate upstream (Ru) and downstream (Rd) reaches, and in the more distant U and D study sites.

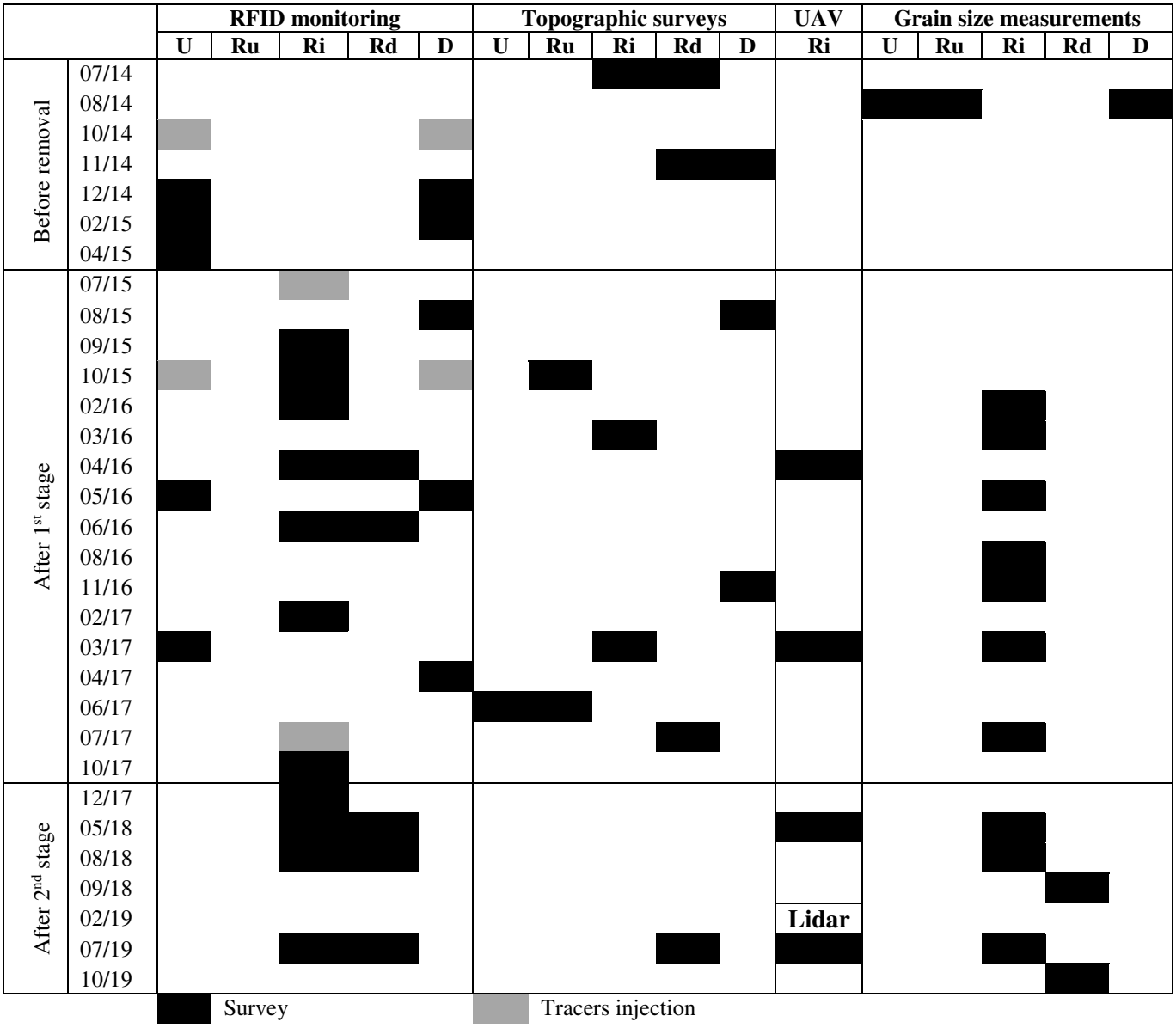

4.2.2 Aerial photographs taken by an unmanned aerial vehicle and SFM photogrammetry

To more accurately assess the volumes involved in the two dam removal stages, a 3D reconstruction of the entire reservoir was also carried out using aerial photographs taken by an unmanned aerial vehicle (UAV). The use of photogrammetry is increasing to characterize river responses in restoration or rehabilitation projects (Ritchie et al., 2018; Marteau et al. 2020, a, b). At Pierre Glissotte, four overflight sessions of the site were conducted, in April 2016, March 2017, May 2018 and July 2019. In 2019, a large area was covered by vegetation during our overflight session, so we used Lidar data to survey our study site. The data are from an airborne Lidar campaign that was carried out in winter 2019. The first drone sessions were carried out

with a Sony RX1 camera mounted on a hexacopter UAV and the last three with a DJI Mavic Pro. The reconstruction was based on the structure from motion (SfM) photogrammetry method (Fonstad et al., 2013). Agisoft Metashape (v1.5.2) software was used to process the photographs. This produces a 3D point cloud (about ten million points preserved after decimation of the point cloud) from which a very high resolution (0.05 m) digital surface model (DSM) is generated directly in Agisoft Metashape. The Canupo algorithm (Brodu and Lague, 2012) was then used to filter out the areas colonized by dense vegetation. The number of ground control points (GCPs) in each flight session is listed in Table 3. For practical reasons, it was impossible to keep fixed GCPs in the field but GCPs were surveyed by a Trimble Total Station. Particular attention was paid to respecting a homogeneous spatial distribution of GCPs (Rangel et al., 2018), and 30% were used as independent checkpoints (Sana-Ablanedo et al., 2018). The characteristics of each flight session and the associated errors after bundle adjustment are given in Table 3. Checkpoints' vertical RMSE were used to evaluate uncertainties in calculating volumes and minimum levels of detection (Schaffrath et al., 2015) at the 95% confidence interval ($LoD_{95\%}$) of the DSMs of difference according to the formula $LoD_{95\%} = \pm 1.96 \times \sqrt{RMSE_{Year}{}^2 + RMSE_{Year-1}{}^2}$.

Table 3. Characteristics of the UAV campaigns in the former Pierre Glissotte impoundment and details of the respective SFM processing.

Date	UAV	Ground Sample Distance (GSD) (cm)	Number of GCPs	Number of checkpoints	RMSE V (m)	RMSE H (m)
20/04/2016	Hexacopter with Sony RX1 camera	1.07	12	5	0.01	0.025
20/03/2017	DJI Mavic Pro	1.1	11	5	0.04	0.025
02/05/2018	DJI Mavic Pro	1.1	17	8	0.033	0.055

As the topography of the reservoir was not available just before it was emptied, the pre-removal topography was reconstructed by virtually filling in the newly opened channel and the volume of this infilling was

calculated. To this end, the slope of the valley was detrended using the average slope of the new channel bottom and a plane with an elevation corresponding to that of the bankfull level was created (Thommeret et al., 2016). By subtracting the bankfull level from the detrended DSM, the volume of sediment evacuated between July 2015 and April 2016 was calculated. For subsequent surveys, the DSM in year T was subtracted from the DSM in year T-1. This meant the deposition and erosion zones could be located and the corresponding volumes calculated with the associated estimated error. In 2019, Lidar data comes with a vertical accuracy of 10 cm. Another uncertainty associated with the sediment volume in general is due to the fact that sediments under the water surface are not included in the calculation of volume. Considering our aerial photographs were always taken during low flow and the bypassed configuration of the former impoundment since March 2016, water height was similar in each campaign and can be considered as close to the profile of the river bed. Consequently, significant sediment dynamics under water could still be identified when the water surface altitude varied. However, slight local sediment dynamics may not have modified the water surface altitude and consequently may have gone unnoticed. In all cases, we considered the volume of sediment underwater to be negligible.

Finally, using the DSM obtained after each session of aerial photography by UAV, the longitudinal profile (water surface) of the river in the former impoundment could be reconstructed each year between 2016 and 2019.

4.2.3 Grain size distribution

At all the study sites, the grain size distribution of the riverbed was determined using the surface sampling method proposed by Wolman (1954). Between 2016 and 2019, at the Pierre Glissotte impoundment, three gravel bars were sampled at least eight times (100 particles per bar on each occasion). The bars sampled are located in the upstream, intermediate and downstream parts of the old reservoir (supplementary material, Fig. S4). In 2018, a sampling site was added about 160 m downstream from the Pierre Glissotte dam. There, 100 particles were sampled and measured in September 2018 and October 2019.

5. Results

5.1 Adjustments in the former reservoir

5.1.1 Channel morphodynamics

Monitoring first highlighted the rapid response of the river as soon as emptying began. Although performed at low discharge, it carried away a large quantity of fine sand and silt sediments. Barely more than a week after the water level was lowered, a first steep slope failure (knickpoint) was identified 40 meters upstream of the dam (supplementary material, Fig. S5, July 28, 2015). Within eight days, the incision had already dug a channel more than 1.50 m deeper downstream of the knickpoint. A lesser incision (average 0.45 m) was also cut into the reservoir deposits upstream of the knickpoint for approximately 160 m. By March 2016, the knickpoint had already passed the tail of the reservoir and reached the bypassed section upstream, reaching more than 400 m up the Yonne in the space of eight months. At that point in time, the width ranged between 6.5 and 19.5 m and the maximum bankfull height was over 4 m (median value: 2.1 m) (Figs. 3 and 4, and supplementary material, Fig. S5). The formation of an average 16-m wide and 2.3-m deep channel resulted in the remobilization of 26% of the volume of sediment contained in the reservoir, i.e. 11,039 m^3 of mainly sandy material (Fig. 4, Table 4) (Gilet et al., 2018).

From summer 2016 on, we observed a weakening of the intensity of the erosive processes and the progressive stabilization of the new morphological and sedimentary conditions shaped in the reservoir (Figs. 3 and 4).

During this period, channel widening continued at a lower rate, mainly through lateral erosion and bank undermining. The slowing down of vertical erosion is accompanied by the coarsening of the material in the new riverbed (see section 5.1.3) but also by the revealed presence of local grade controls in the longitudinal profile. The main control was obviously the remaining 4 meters of the dam that controlled the entire new profile formed ("New local base level" (1), Fig. 3) but there were also an outcrop of bedrock and many multi-decimetric boulders ("Grade controls", Fig. 3) that prevented or slowed down bed incision.

Ultimately, a total volume of 951 m^3 was released into the system between April 2016 and March 2017, much less than the 11,039 m^3 eroded in the preceding nine months (Fig. 4, Table 4). The calculation of volumes even showed the formation and stabilization of certain deposits (263 m^3 accumulated sediment)

mainly corresponding to three large gravel bars on which the sediment size was measured (supplementary material, Fig. S4). This stabilization was accompanied and potentially favored by plant colonization of the deposits during this period.

After the second stage of the removal (October 2017), significant vertical and lateral erosion occurred again (Figs. 3 and 4). Seven months later, 4,180 m^3 of gravel-sand sediment had been eroded and reinjected into the river system (Table 4). A significant proportion of this release was the result of both river action and mass movement that affected the banks. Figure 4 shows that erosion was particularly concentrated in a stretch 170 m in length immediately upstream of the former dam. Nevertheless, small areas of significant erosion can also be seen in the middle of the former reservoir. Also, the important aggradation that can be seen on Figure 4 near the dam (dark green area) is artificial. Sediments were excavated to form the new channel passing through the hole in the dam and stocked against the right hillslope of the valley (also visible in supplementary material, Figs. S2 and S5, photograph taken on November 16, 2017). A comparison between the 2018 and 2019 profiles shows that the bed was not completely fixed (Fig. 3). Some sectors were incised and others were in a state of aggradation, even if the differences in altimetry were moderate (a few tens of centimeters). These moderate changes were confirmed by the differential DSM between 2018 and 2019 (Fig. 4). The sediment volumes calculated from it were 597 m^3 of eroded sediments for 603 m^3 of aggraded sediments (Table 4). These numbers suggest a slowdown of morphogenic activity but not the complete stabilization of the fluvial system. Eventually, 34% of the reservoir fill was eroded and exported downstream of the dam (Table 4).

Table 4. Sediment budget in the reservoir between each photogrammetry campaign.

Difference of DSM (DoD)	Eroded volume (m^3)	Deposited volume (m^3)	Sediment budget (m^3)	Rate (m^3/d)	Part of reservoir fill[1] exported downstream the dam (%)
$DoD_{2016-2015}$	11 039±59	0	-11 039±59	-40	25.9
$DoD_{2017-2016}$	951±154	263±77	-688±231	-3	1.6
$DoD_{2018-2017}$	4 180±195	1355±76	-2825±271	-7	6.7
$DoD_{2019-2018}$ (2019 from Lidar)	597±173	603±375	6±548	0.01	-

1: based on the sediment volume (42 600 m^3) calculated in Gilet et al. (2018).

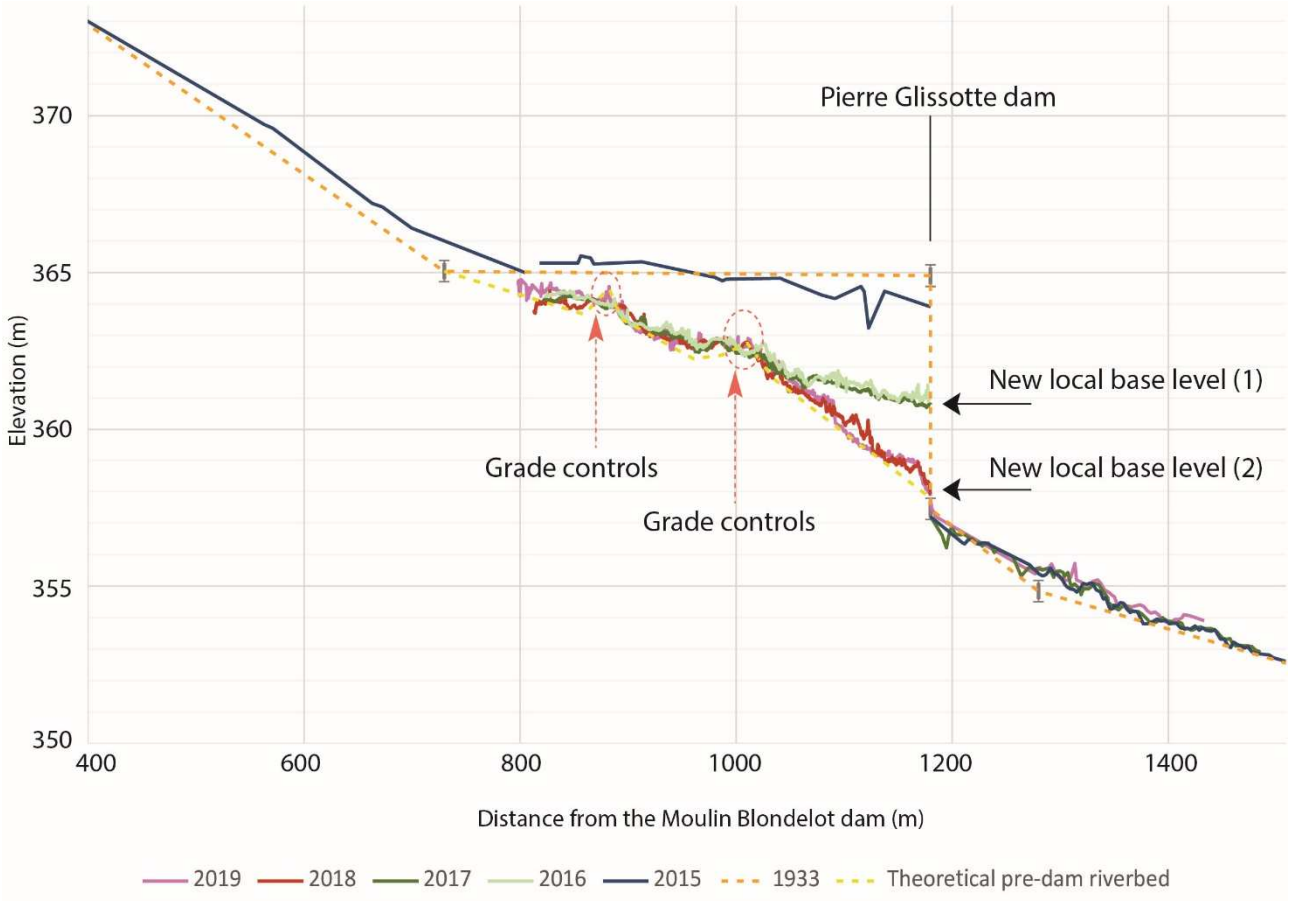

Fig. 3 Development of the new Yonne long profile around the Pierre Glissotte dam.

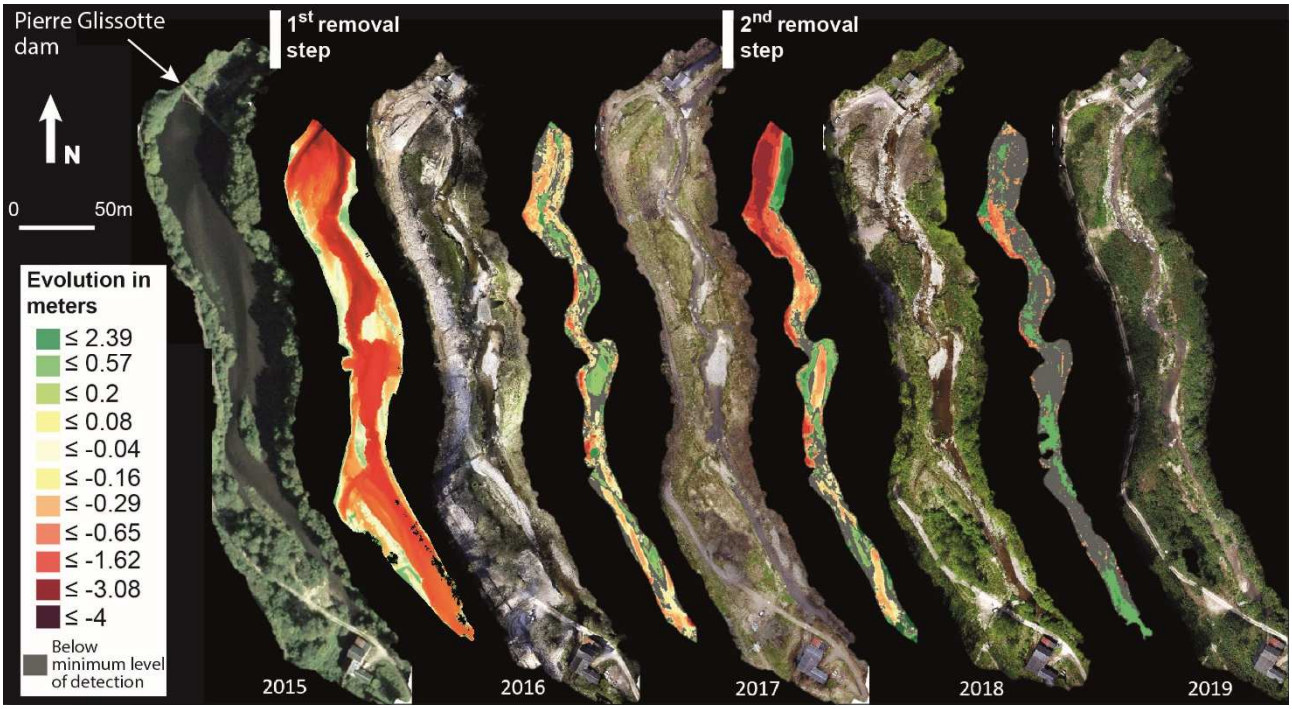

Fig. 4 Planimetric and vertical changes in the former reservoir (DSM) between each aerial photograph campaign by UAV (except 2015, IGN, ortho database). The minimum level of detection is set at the 95%

confidence interval ($LoD_{95\%}$) of the DSMs of difference, described in section 4.2.2. The intervals of the vertical evolution correspond to a manual classification.

5.1.2 Coarse bedload transport

Figure 5 shows the movement of the tracers over time and with respect to the hydrology. For each survey, the mean inter-survey distance (Fig. 5A) of the detected tracers corresponds to the mean distance traveled since the previous survey (or to injection in the 1st survey). Mean inter-survey velocity (Fig. 5B) is the ratio between the mean inter-survey distance and the time elapsed since the previous survey.

RFID tracking showed that the coarse load (pebbles and cobbles) stored at the tail end of the reservoir was very quickly set in motion again during and after the first removal step. The first two tracer displacement surveys were carried out two and three months after the start of the removal (emptying phase included). They revealed very high bedload displacement rates, with a mean inter-survey velocity equal to 138 m/year and 347 m/year respectively. This very rapid movement was observed despite the absence of a noticeable peak flow.

The remarkable morphogenic activity in the first nine months following the first removal phase is clearly visible when the results of the bedload tracers at Pierre Glissotte are compared with those at the undisturbed sites, U and D (Fig. 5A-B). The distance is shorter and the velocity recorded at the control sites in the same period is significantly weaker: e.g., the bedload velocity was 36 m/year at U, and 71 m/year at D, between April 2015 (U) - August 2015 (D) and May 2016. Also, for comparable hydrological conditions during the 9 months following the first removal step, bedload displacements appear more important at Pierre Glissotte. Between February and June 2016, a first decrease in the mobility of the Pierre Glissotte tracers was observed but the mean displacement velocity was still high (Fig. 5B). In total, between the 1st injection and June 2016, the mean distance travelled by mobile tracers was 123 m (134 m/y) (Fig. 6, photographs 1-2).

The relative morphological stability observed from summer 2016 was accompanied by a major slowdown of the bedload transport (Fig. 5): the mean distance covered by the mobilized tracers between June 2016 and February 2017 was 17 m (25 m/year), despite the occurrence of multiple flood events during that time interval (Fig. 5).

The bedload was again significantly mobilized following the second removal step. The new tracers injected (2nd series) into the channel a few months before the complete opening of the dam were mobilized and some travelled several hundred meters in about 13 months (Fig. 6, photographs 3-4). Between October 2017 and

August 2018, the inter-survey particle velocity increased again (for the 3 RFID surveys in this time interval, a mean value of 169 m/year for the mobile tracers of the second injection and 67 m/year for those of the first). However, it remained lower than those recorded after the first removal step (up to 340 m/year) (Fig. 5B). This time, the high velocity of bedload did not slow down after the first year following the removal step but continued for at least one more year, despite the exit of the fastest tracers from the survey area (Fig. 5B). Our final survey carried out in July 2019 revealed displacement of 209.5 m on average for the tracers mobilized since August 2018 (considering the two series of injections together). This corresponds to a mean velocity for the two injections of 241 m/year (series 1) and 238 m/year (series 2).

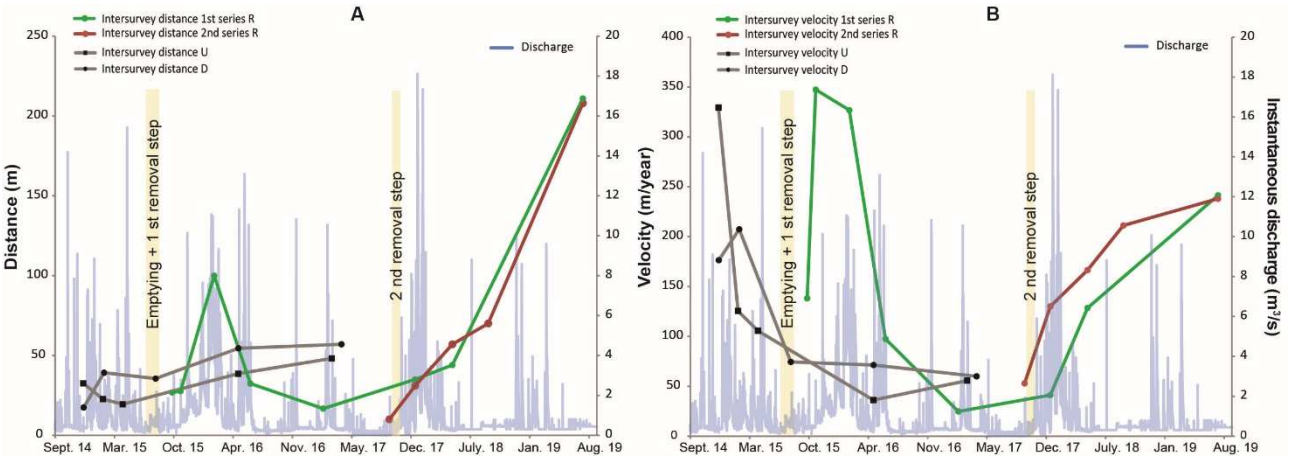

Fig. 5 Bedload displacements at Pierre Glissotte (R) and at the study sites undisturbed by the removal (U, D). A. Mean inter-survey distance covered by the mobile tracers. B. Mean inter-survey velocity of the mobile tracers. *For each survey, the mean inter-survey distance (A) of the detected tracers corresponds to the mean distance traveled since the previous survey. For each survey, mean inter-survey velocity (B) is the ratio between the mean inter-survey distance and the time elapsed since the previous survey.*

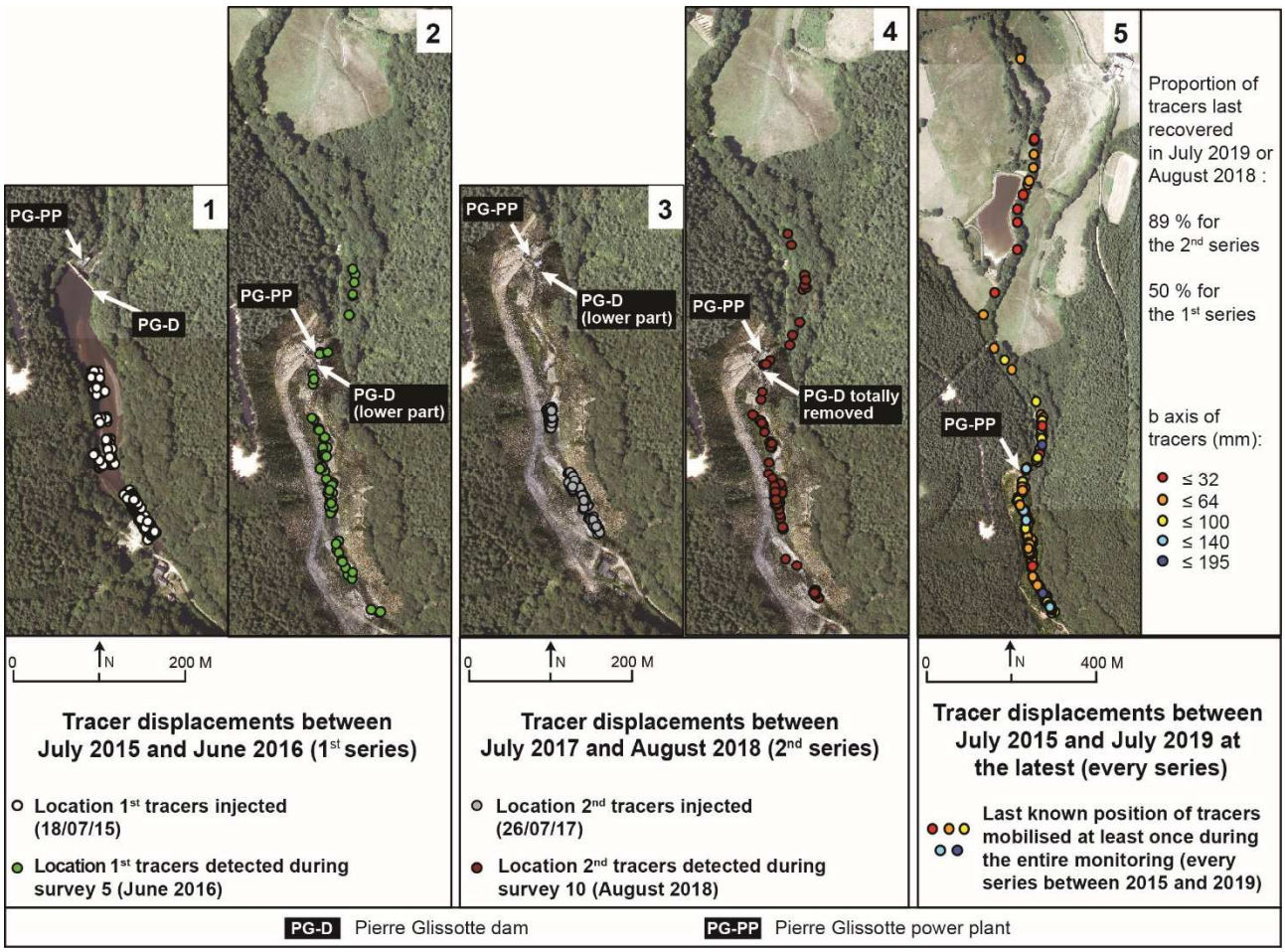

Fig. 6 Positions of RFID tracers at different phases of the Pierre Glissotte removal.

5.1.3 Bed texture

The riverbed of the new channel that formed after the first removal works was rapidly covered with coarse sediments coming from the reservoir tail and the upstream reach. By February 2016, the sandy bed had completely turned into a gravel bed (D_{50} = 37 mm) (Fig. 7A). The bed adjustments and the size of the substrate particles (D_{50} and D_{90}) continued to increase until August 2016 (Fig. 7), confirming the gradual restoration of coarse bedload transport in the former reservoir. A change in sediment dynamics was then recorded as a reduction of the median size of the particles was measured on the three main bars in the former reservoir between August 2016 and February 2017 (Fig. 7A). After the second removal step, the changes in the size of the particles comprising the gravel bars were less uniform (Fig. 7); the increase in the D_{50} was generally maintained until May 2018 (August 2018, in the upstream part), after which there was a decrease in the D_{50} in the sampled bars until July 2019. This is similar to the decrease measured between August 2016, about one year after the first removal step, and February 2017. It should be noted that the 2018

decrease in median diameter was particularly strong in the case of the downstream bar (Fig. 7A) when its D_{90}, which had changed very little after the first stage of work, increased very rapidly from September 2017 on (Fig. 7B). This downstream bar thus appeared to be becoming more heterogeneous, probably due to the departure of its intermediate size fraction.

All indicators suggest that in summer 2019, the bed was not yet stabilized and still in search of equilibrium conditions. Indeed (i) the size of the pebbles on bars was still evolving and remained below the D_{50} of the uninfluenced sites (U and D) (Table 1); (ii) the transport velocities recorded in spring-summer 2018 and summer 2019 were still high; and (iii) certain bars apparently stabilized before the second removal stage was in erosion again. Finally, the active adjustment observed after the second step was less spectacular but lasted longer than after first removal step.

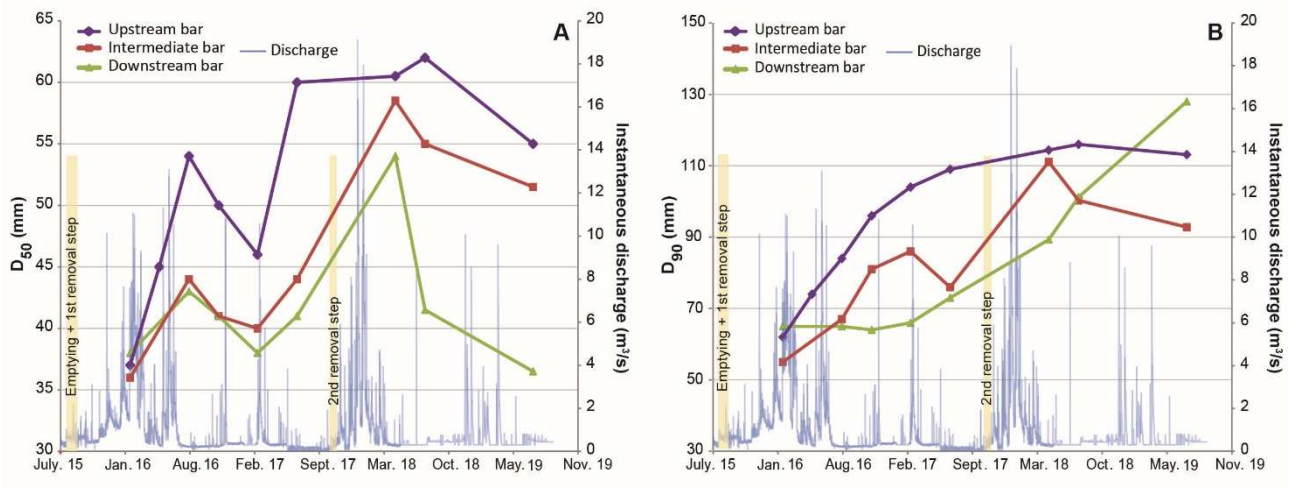

Fig. 7 Changes in grain size distribution of three gravel bars located in the former Pierre Glissotte reservoir. A. Changes at D_{50}; B. Changes at D_{90}.

5.2 Changes in the downstream reach

5.2.1 Fine deposits

In July 2015, the butterfly valve got stuck in open position as soon as the reservoir began to empty, very quickly releasing a massive amount of sand and silt even before the top part of the dam was removed. The resulting concentered flow of highly suspended sediment significantly affected the aquatic biocenosis for at least 3.5 km downstream, and probably as far as Pannecière reservoir, 5.5 km further downstream. Sandy deposits up to 40 cm thick formed along the river course, primarily on the channel margins. Even if this

490 event probably had a strong impact on the aquatic communities, from a morphological point of view, the
491 impact was slight. Indeed, the sand bars were ephemeral as they were rapidly evacuated during the following
492 2015-2016 high waters of the hydrological season. By June 2016, they had almost disappeared, and the
493 thickness of the remaining patches had been greatly reduced.
494
495 **5.2.2 Bedload continuity**
496
497 Due to the high bedload dynamics mentioned in the previous sections, sediment continuity was quickly
498 restored. As early as June 2016, about ten tracers injected (5% of the injection) into the former reservoir
499 were found scattered over more than 100 m downstream of the former Pierre Glissotte dam (Fig. 6,
500 photographs 1-2). The number of tracers found downstream then increased slightly until the beginning of the
501 second stage of removal (12 tracers were detected downstream the dam in February 2017). After this stage
502 and the renewed sedimentary dynamics it triggered, an increasing number of tracers continued to be detected
503 in the downstream section. By August 2018, at least 29 tracers (13% of all the tracers recovered) had gone
504 beyond the former dam, spread over a distance ranging from 4 to 420 m downstream of the old structure.
505 One year later, in July 2019, this figure reached a minimum of 53 tracers (26% of the recovered tracers),
506 over a river course extending up to 850 m downstream of the dam (Fig. 6, photograph 5), at the exception of
507 one isolated head tracer located 1400 m downstream of the dam. These tracers were distributed fairly evenly.
508 No preferential storage areas really emerged, except for a local sector located 95-125 m downstream of the
509 former dam, immediately downstream of the confluence with the hydropower plant tail race, where the
510 channel widens. Apart from this specific area and a few tracers that appeared to be stuck behind blocks, the
511 particles that passed through the former reservoir remained highly mobile and did not settle downstream of
512 the structure.
513
514 **5.2.3 Morpho-sedimentary adjustments**
515
516 A comparison of the long profile before the removal of the dam with those surveyed in 2017 (after the 1st
517 stage) and in 2019 (after the 2nd stage), over a length of 315 m downstream from the dam, confirmed the
518 absence of significant deposits and generalized bed elevation (Fig. 3). The vertical variations are rather
519 positive, indicating the formation of small gravel deposits. However, in the last survey in 2019 they were still
520 fairly limited (< 30 cm). These small bars, or rather gravel and pebble patches, were actually more present

between 2017 and 2019 than after the first stage of the restoration operation. Comparison of cross-sections surveyed in 2014, 2017 and 2019 confirm our observations up to 2019 (Fig. 8, see also Fig. 2 for location). The morphological changes consisted mainly in a few areas of limited aggradation (< 40 cm). These aggraded sections were mainly either on median or mid-channel bars that already existed before the dam was removed (Fig. 8A), or near the banks (Fig. 8F). Also, like the long profile, some vertical adjustments appear to have continued between 2017 and 2019 (Fig. 8A, 8C, 8F). Some changes are still complex to interpret as cross-sections show both aggradation and bed degradation (Fig. 8C), changing dynamics (Fig. 8D) or an almost unchanging situation (Fig. 8E). Considering the substrate, the comparison of two surface grain size campaigns carried out 160 m downstream of the former dam, in September 2018 and October 2019, tends to underline the limited nature of the textural adjustments: the D_{50} only increased from 73.5 to 79.5 mm and the D_{90} decreased from 250 to 241 mm.

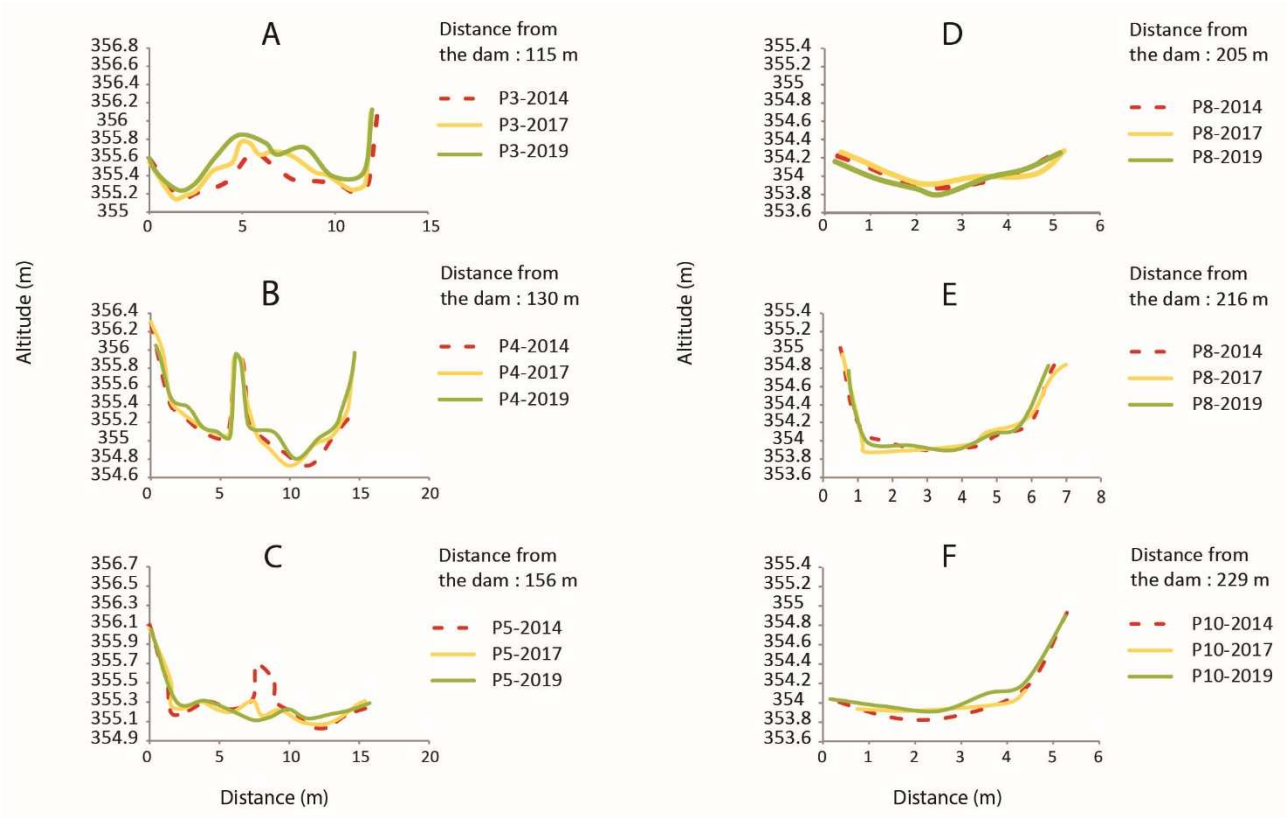

Fig. 8 Series of cross-sectional profiles downstream of the former Pierre Glissotte dam (Rd sub-reach) in 2014, 2017 and 2019.

6. Discussion

6.1 Adjustments in the former reservoir

Figure 4 shows that most of the morphological changes mentioned above were observed over a fairly short period of time, with the most important morpho-sedimentary adjustments occurring after the first step of the removal operation. A comparison of the adjustments observed on the Yonne river with those of other removal operations underlines the speed of the erosive process at work at Pierre Glissotte (Fig. 9). Over the first 9 months following the start of the dam removal, the erosion rate measured at our study site (26%) was higher than almost all the cases corresponding to a multi-stage removal in Figure 9 (except the one in Brownsville), much faster than that of the two other reservoirs with comparable grain size composition (Rockdale Dam and La Valle dam; Doyle et al., 2003), and very close to the Brownsville dam removal characterized by much coarser sediments (D_{50} = 59 mm) (Walter and Tullos, 2010). After this first very rapid erosion phase that lasted a little less than a year, the evolution of the erosion rate is non-linear. The readjustment of the newly formed channel in the former reservoir corresponds indeed to a transient system that Bellmore et al. (2019) associated with "dynamic and non-linear recovery trajectories". The morphogenic acceleration phases are the direct consequence of the two deconstructing works that lower the control base level by several meters. Once the equilibrium profile is almost restored, the system slowdowns and the morphogenic activity decreases. This relay phenomenon has been described in the literature notably by Pizzuto (2002) and by Pearson et al. (2011). The intense erosive phase, a process-driven system due to morphological instability, is then followed by a gradual transition leading to a more classical functioning of the river system with a larger role played by the hydrological episodes ("event-driven system") (Pearson et al.; 2011; Collins et al., 2017). In Pierre Glissotte, close to what Pearson et al. (2011) had already noticed, large floods appeared to play a major role in the most incised sections, in mobilizing the impounded sediments that emerged during base flow, and in maintaining bank undermining in the widest areas.

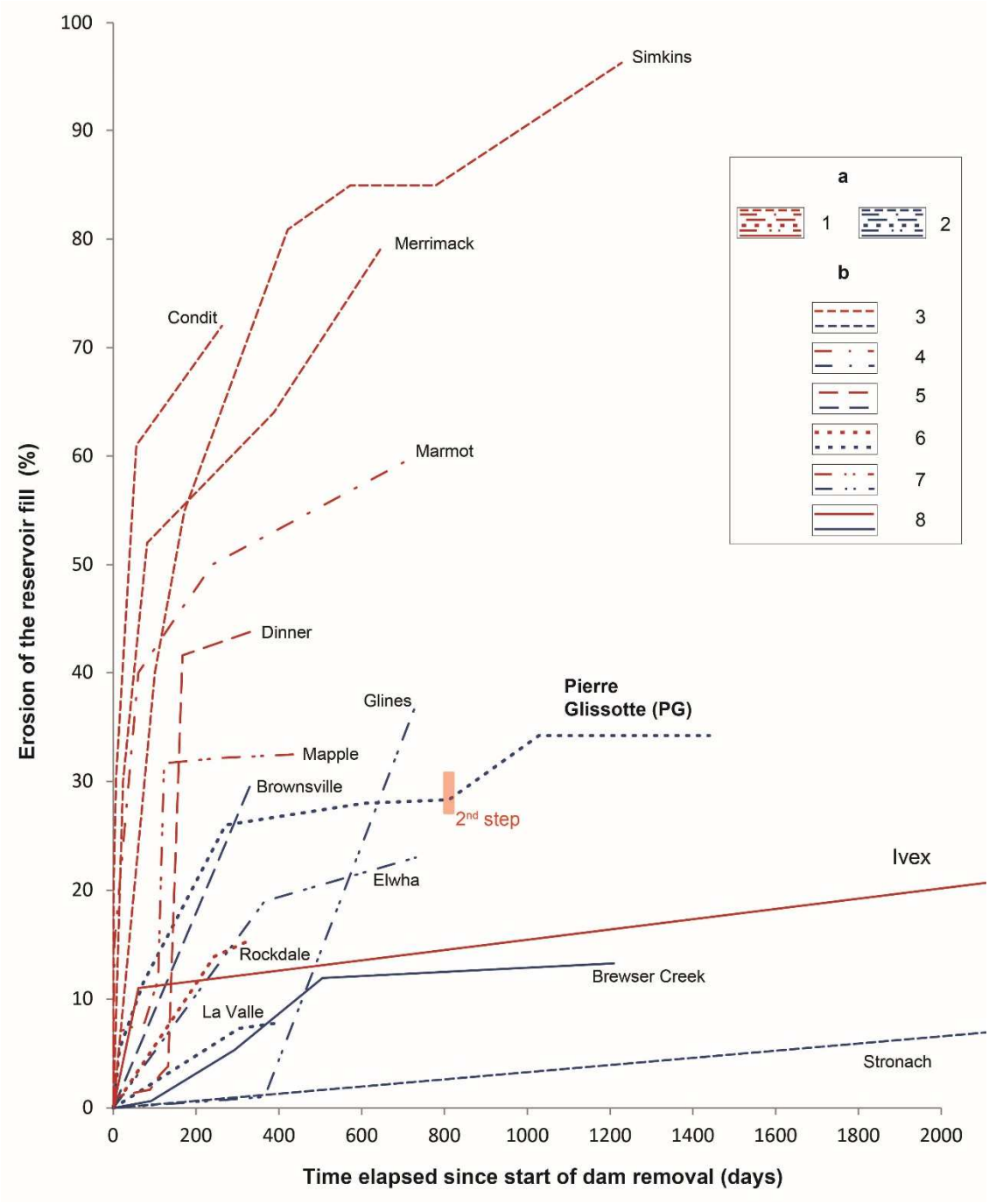

Fig. 9 Comparison of the erosional velocity of reservoirs following removal projects (Sawaske et Freyberg, 2012; Lewis et Grant, 2015, modified). *After: Doyle et al., 2003; Stewart, 2006; Evans, 2007; Straub, 2007; Burroughs et al., 2009; Walter & Tullos, 2010; Pearson et al., 2011; Major et al., 2012; Randle et al., 2015; Collins et al., 2017).*

a. Type of dam removal: 1. Rapid removal; 2. Staged removal; b. Main sedimentary composition of the reservoir; 3. Dominance of sands; 4. Non-cohesive mixed sediments (sands and coarse material); 5. Coarse material (> 2mm); 6. Mixed fine sediments (sand, mud); 7. Mixed sediments (mud, sands and coarse material); 8. Mud.

A closer look at the Pierre Glissotte situation shows that the very rapid erosion that occurs in the reservoir directly after the lowering of the 3 upper meters of the dam is favored by the non-cohesive nature of the

578 sediments. The rather young (less than 40 years old) filling of the reservoir was indeed characterized by an
579 alternation of sandy deposits with finer layers rich in organic matter. This allowed the rapid formation of a
580 channel that enlarged due to the upstream displacement of a mobile knickpoint. These types of knickpoint
581 have frequently been described in the literature (Pizutto, 2002; Doyle et al., 2003; Stewart, 2006; Major et
582 al., 2012; Magilligan et al., 2016; Ibisate et al., 2016). They allow regressive erosion and favor the incision
583 of the bed despite low flows, such as that observed on the Yonne River in summer and autumn 2015.
584 Consequently, the hydraulic capacity of the channel increases and the peak flow of the following hydrologic
585 season continued the vertical and lateral erosion processes. The process of bank destabilization (widening)
586 after the first stage of incision is also consistent with what is reported in the literature (Cantelli et al., 2004;
587 Pizutto, 2002; Pearson et al., 2011; Major et al., 2012; Randle et al., 2015; Ibisate et al., 2016). Until autumn
588 2016, the morphological response in the former impoundment may for instance partially be integrated in the
589 five-stage readjustment model proposed by Doyle et al. (2003): A) pre-works; B) lowering of the water level
590 and differentiation between the new bed and the outlet channel; C) incision; D) incision and widening; E)
591 aggradation and widening. F) state of near equilibrium. The first 4 stages clearly took place during the first
592 year of monitoring at Pierre Glissotte, but stages E and F were not achieved. A slower and more local
593 incision and some local widenings continued until the second removal step in October 2017. Our
594 observations comfort the proposals made by Evans (2007) to adjust the model of Doyle et al. (2003) by
595 adding a phase E' corresponding to the stabilization and revegetation of the deposits. Indeed, this stage
596 started to occur in late spring 2016, on some stable gravel bars, and fine deposits collapsed or slumped from
597 the banks. As in the Ivex reservoir (Evans, 2007), these stable deposits were located near the foot of a
598 previously unstable bank and often faced the opposite bank subject to undermining and prone to erosion
599 and/or collapse (i.e. in places where the channel widened).
600
601 Following the reactivation of bedload transport, the formation of the channel was accompanied by an
602 increase in the particle size of the bed substrate, again in accordance with what has been observed in other
603 cases of dam removal (Pearson et al., 2011; Major et al., 2012). A shift from fine (< 2 mm) or slightly coarse
604 (< 8 mm) grain size to a gravel bed was, for instance, observed in the Souhegan River (Pearson et al., 2011)
605 following the removal of Merrimack Dam. Though at the Merrimack Dam, a stage of refinement was
606 initially observed over the 300-350 m stretch upstream of the dam. At Pierre Glissotte, all the coarse

607 fractions present at the tail and in the reservoir were very quickly remobilized and travelled the entire length
608 of the reservoir (400 m) in just a few months (Fig. 6, photographs 1-2).
609 When considering these high transportation rates recorded at Pierre Glissotte (R), one could argue that they
610 were also recorded at the control sites (U and D) just after the injection of marked particles (Fig. 5B). Indeed,
611 the literature suggests that the mobility of tracers after their injection may be favored by an artificial
612 protruding or unconstrained position (Gintz et al. (1996) in Lamarre and Roy, 2008 and Houbrechts et al.,
613 2015). Some studies over longer time scales (several years), have also shown that the propagation rates of
614 marked particles diminished over time (Ferguson and Hoey, 2002; Haschenburger, 2011, Houbrechts et al.,
615 2015). However, at Pierre Glissotte (R), it is important to note that: (i) the first bedload displacements
616 occurred with the absence of a flood event; (ii) the high transport rate lasted much longer and (iii) the
617 cumulative distance reached in the former reservoir (123 m in 9 months for the first tracer series) increased
618 much faster than at the control sites (50 m in 6 months at U, and 60 m in 9 months at D, following the tracer
619 injections and under hydrological conditions that are comparable or even more favorable to mobility). In this
620 case the rapid bedload displacements were clearly favored by the removal and specific conditions of the
621 reservoir. First the lowering of the base level and the migration upstream of the knickpoint that destabilized
622 the bed. Second, the sandy nature of the bed facilitated the incipient motion of the pebbles and cobbles
623 because of a protrusion effect and the reduction of the friction angle (Wilcock et al., 2001; Miwa and Parker,
624 2017; Dépret et al., 2020). This highlights once more the important role of sand in the river response. Even
625 though this study is intentionally focused on the bedload of the Yonne River (pebbles and cobbles), it may be
626 worthwhile to further assess the sand dynamics and transport rates. Finally, it is interesting to note that the
627 intense morphogenic activity is responsible for the rapid incipient motion of coarse bedload and changes in
628 bed texture (coarsening) that eventually induced a retroactive loop that slowed down the system. The
629 coarsening of the bed progressively limits the sediment transport and decreases the morphogenic activity.
630 The same cycle of intense adjustments followed by the slowing down of erosive activity was observed after
631 the second step of the removal (Fig. 9), though the adjustments recorded were more limited and the active
632 phase was shorter. This may be explained because the channel substrate was coarser but also because of the
633 appearance of large boulders that play the role of local base level. These blocks are multi-decimetric to
634 metric and, together with some bedrock outcrops, slowed down the vertical erosion. Indeed, other studies
635 have shown that these hard areas (or other materials that are more cohesive and resistant than the previously

636 eroded layer) can limit incision and regressive erosion (Pearson et al., 2011; Wilcox et al., 2014; Gartner et
637 al., 2015; Warrick et al., 2015; Ibisate et al., 2016), and by fixing the bed, may isolate the surrounding
638 sediments of the reservoir (Major et al., 2012).
639 These results, like those of Straub (2007) on Brewster creek, emphasize the fact that to understand the multi-
640 stage changes consecutive to the removal of the dam, high frequency measurements are needed (Table 2).
641 This is clearly visible on Figure 9. On one hand, the volume eroded from the Ivex (Evans, 2007) or the
642 Stronach (Burroughs et al, 2009) was assessed over 10 and 12 years respectively but only from one
643 (Stronach) or two (Ivex) surveys. In consequence, the erosion in these reservoirs may not have been as
644 regular as it may seem, despite the fact that these dams were removed in one step. On the other hand, the
645 non-linear dimension of the recovery trajectory in the former Pierre Glissotte reservoir is well shown on
646 Figure 9. Our study emphasizes the gradual establishment of the regenerative processes that are targeted in
647 river restoration (Hart et al., 2002). Indeed, the succession of different stages with changing morphogenic
648 activity corresponds to the progressive shaping of a new channel along a 400-m long stretch, with lotic
649 conditions and varying width, depth and slope. It also corresponds to new sediment deposits of variable
650 stability, and to the discovery of bedrock outcrops and boulders. All these changes in geometry and textural
651 conditions lead to clearly diversified plan forms (channel side, mid-channel and point bars, sinuous sections,
652 straight and plane bed sections), changes in substrate grain-size and sedimentary units, and in hydraulic
653 conditions (pools, runs, two 15-m long rapids). In the former Pierre Glissotte reservoir, the restoration of
654 sediment continuity and bedload transport is clearly associated with the restoration of hydromorphological
655 and ecological functioning, which was one of the objectives of the project.
656
657 **6.2 Very weak adjustments in the downstream reach showing poor resilience of the system**
658
659 Except for the temporary deposits of sand following the first step of the removal in July 2015, no significant
660 change in the bed geometry, in the fluvial planforms or in the substrate grain size appeared downstream of
661 the former Pierre Glissotte dam during the first three years of this study. This absence of reconfiguration
662 contrasts with the intense morphogenic activity described in the reservoir.
663 The initial deposits of fine sediment in the center of the channel were quickly evacuated and, as already
664 described in the literature (Doyle et al. 2003; Draut and Ritchie, 2015), only the lateral margins of the

channel remained covered for a few months by centimeters-thick deposits. This constitutes only a "short-term response" (Foley et al., 2017a) to the first step of the dam removal and the absence of other deeper morphological changes was unexpected. Grant and Lewis (2015) have for instance underlined that downstream of the Marmot dam, if sands were rapidly evacuated over tens of kilometers, the gravels were massively deposited only a few kilometers downstream of the dam (Major et al., 2012). Pierre Glissotte is smaller but the rapid transfer of bedload towards the downstream reach suggested that something similar could happen here. The reaction time downstream of the dam is already rather long given the fact that the bedload supply was reactivated years ago and that the fastest particles are now located hundreds of meters downstream. The weak evolution shown by the last topographic surveys raises the question of whether the limited morphological changes may be the result of limited bedload supply (despite the sediment continuity being restored) or the result of its high dispersion.

Thanks to the volume of coarse sediment stocked in the reservoir tail (2,300 m^3), the bedload discharge of the Yonne River was calculated. It is 77 or 177 m^3/year depending on whether we consider that the bedload transport stopped in 1985 (the second watering of the dam) or in 2002 (the definitive closing of the bottom outlets), corresponding to a bedload yield of 1.6 or 3.6 t/km^2/yr respectively (i.e. values consistent with those of Houbrechts et al. (2006) in similar Belgian environments). Then, one may consider that between 2,600 and 3,000 m^3 of pebbles and cobbles were reintroduced to the system since the reopening of the river course (bedload trapped in the former reservoir + sediment supplied from upstream). Figure 7 shows that a part of this volume spread out along the entire former reservoir in less than 6 months and UAV photographs allow us to measure the surface of the gravel bars in April 2016, March 2017, May 2018 and July 2019. They are relatively constant, ranging between 2080 and 2530 m^2. The thickness of this gravel deposit ranges between a few centimeters in pools, up to 1 m in the thickest bars. By considering an average thickness of 0.5 m (which is probably overestimated), the volume of the gravel deposited in the former reservoir would range from 1040 m^3 to 1260 m^3 (i.e. between 33 and 50% of the total load). The remaining volume has been totally evacuated from the tail of the reservoir for months and distributed in the downstream reach.

These calculations suggest that a sediment wave occurred consecutively to the removal of the dam. According to the classification of Lisle et al. (2001), this corresponds to a dispersing wave rather than a translating one. The particularity in this case, is that the load spread out in the former reservoir in a thick layer but once it passed the former dam the wave disappeared as the particles were flushed away. It appears

694 indeed from the PIT tag surveys that the bedload that passes the former reservoir transits through the
695 downstream reach with very short resting times, preventing sediment accumulation and bed aggradation. The
696 same observations have been reported following dam removals from the Elwha river (Warrick et al., 2015;
697 Ritchie et al., 2018) and from the fracturing of the Barlin dam on the Dahan river (Tullos and Wang, 2014).
698 In the latter case, deposits increased and altered the longitudinal profile only when the channel lost carrying
699 capacity at the end of a very confined section (Tullos and Wang, 2014). In Pierre Glissotte, it is probably
700 also the narrowness of the valley (confinement) that facilitated the rapid evacuation of the sediment.
701 Moreover, the confinement is reinforced by ripraps present on the left bank. They date from the construction
702 of the first hydroelectric facility in 1927. The structure not only ensures a certain straightness of the river
703 course but also increases the hydraulic capacity of the channel, the water depth at peaks flow and therefore
704 the associated shear stress. Comparing several downstream decommissioning sites, Poeppl et al. (2017) also
705 found that the presence of other anthropogenic developments (including bank protections) inhibit
706 adjustments and tend to preserve the configuration developed under the influence of the dams.
707 Another element, that is partly the consequence of this embankment, may also explain the rapid transit of the
708 bedload in the downstream reach of the dam. It is the fact that the river bed is clogged and paved. This
709 confers a low rugosity at the surface of the bed and favors incipient motion of the particles supplied from
710 upstream (Petit et al., 2005; Gob et al., 2010; Gilet et al., 2020). This pavement of the bed has been favored
711 by the partial channelization of the bed but is a direct consequence of the presence of the dam which limited
712 or even stopped bedload transport for decades.
713 So far, these sedimentary characteristics have not been modified by the restoration of the sediment
714 continuity, and the channel geometry and the bedforms remain almost unchanged. The recovery of bedload
715 supply without the morphological reconfiguration of the bed raises questions about the capacity of the
716 restored system to really change its hydromorphological functioning and return to a pre-dam situation (Foley
717 et al., 2017a). In particular, it calls into question whether the restoration of sediment continuity may
718 compensate for the impact of decades of sediment deficit. The morphology inherited from the dam was
719 largely the same four years after the removal started, suggesting the possible irreversibility of this influence
720 and a lack of resiliency. With this in mind, it may be more appropriate to describe the operation as a
721 rehabilitation process, rather than a restoration process (Dufour and Piégay, 2009). Downstream of the Pierre
722 Glissotte site, the paved section showing a deficit in medium-sized load is not very long and consequently

723 the absence of morphological adjustment is probably not worrying from an ecological point of view (macro-
724 invertebrate habitats, substrate and hydraulics of spawning areas, etc.). However, when the unbalanced
725 sections are more extensive, the lack of morpho-sedimentary reconfiguration may turn out to be ecologically
726 problematic.
727
728 **Conclusion**
729
730 The various morpho-sedimentary changes observed in the former reservoir during the four years of
731 monitoring underline the changing nature of the adjustments, their pace and control mechanisms. The initial
732 destabilization process associated with the propagation upstream of the knickpoint led to very rapid
733 readjustments. The new conditions (hard points, more cohesive lower deposits) revealed by the incision and
734 the achievement of more or less transient equilibrium conditions slowed down the morphological changes.
735 These changes are in line with what has been observed for other dam removals. However, in the case of
736 multi-stage removal, it is quite exceptional that 26% of the trapped sediment was re-injected into the system
737 at the end of the first year of restoration such as observed at Pierre Glissotte. This is undoubtedly linked to
738 the nature of the filling (unconsolidated sand and silt) and to the dynamic character of sediment transport in
739 the Yonne river. The reintroduction of coarse sediment into the system slowed down the morphological
740 adjustments, without completely stabilizing the system. The complete lowering of the dam during the second
741 stage of work revived the adjustment dynamics which, almost two years later, are still in progress.
742 At first glance, the absence of major morphological changes downstream of the dam, four years after the start
743 of the work, is quite surprising. It testifies to the possibility that a largely effective restoration of the coarse
744 sediment continuity will not be accompanied by significant morphological readjustment downstream. The
745 bedload reached this downstream section but did not settle there. The influence of the geomorphological
746 context (narrow valley with a steep slope) and the legacy of the dam itself (bank ripraps, straight channel and
747 paved substrate) help to explain the rapid transit of sediment in the downstream reach. The last topographic
748 measurements (2019) tend to show a slight aggradation in several sections whereas aggradation was only
749 very local in 2017. The next campaigns will enable us to see if this adjustment remains minor or is still in
750 progress. In any case, this long reaction time confirms the relevance of long-term studies after dam removal
751 as the river response needs to be clearly understood and differentiated over several time scales.

Acknowledgments

The authors would like to thank Matthieu Moës and the *Agence de l'Eau Seine-Normandie* (public water agency), for financing this research. We are also very grateful to Jean-René Malavoi and Electricité de France (EDF) as well as the PIREN Seine for the financial support they provided for the purchase of research equipment and for the fieldwork. The acquisition of the Lidar data has been funded by the Regional council of Burgundy and treated with the technical support of GEOBFC and MSH Dijon CNRS-uB3516. We extend our sincere appreciation to the Morvan Regional Natural Park for its interest in our research, to Jonathan Touche for his help in the field, and Daphne Goodfellow and Natasha Shields for their assistance with translation. Finally, we would like to thank the two anonymous reviewers for their constructive comments that enabled the quality of the original paper to be greatly improved.

References

Bellmore, J.R., Duda, J.J., Craig, L.S., Greene, S.L., Torgersen, C.E., Collins, M.J., Vittum, K., 2017. Status and trends of dam removal research in the United States. Wiley Interdisciplinary Reviews: Water 4, e1164.

Bellmore, J. R., Pess, G. R., Duda, J. J., O'Connor, J. E., East, A. E., Foley, M. M., Wilcox, A. C., Major, J. J., Shafroth, P. B., Morley, S. A., Magirl, C. S., Anderson, C. W., Evans, J. E., Torgersen, C. E., & Craig, L. S. (2019). Conceptualizing ecological responses to dam removal: If you remove it, what's to come? BioScience, 69, 26– 39.

Bradley, N., Tucker, G.E., 2012. Measuring gravel transport and dispersion in a mountain river using passive radio tracers. Earth Surface Processes and Landforms, 37, 1034–1045.

Bravard, J-P., Petit, F., 1997. Les cours d'eau, dynamique du système fluvial. A. Colin, Coll. U, Paris, 222 p.

Brodu, N., Lague, D., 2012. 3D terrestrial lidar data classification of complex natural scenes using a multi-scale dimensionality criterion: Applications in geomorphology. ISPRS Journal of Photogrammetry and Remote Sensing, 68, 121-134.

Brunsden D., 1980. Applicable models of long term landform evolution. Zeitschrift für Geomorphologie 36, 16-26.

Burroughs, B.A., Hayes D., Klomp K., Hansen J., Mistak J., 2009. Effects of Stronach Dam removal on luvial geomorphology in the Pine River, Michigan, United States. Geomorphology, 110, 96-107.

Bushaw-Newton, K.L., Hart, D.D., Pizzuto J.E., Thomson J.R., Egan J., Ashley J.T., Johnson, T.E., Horwitz, R.J., Keeley, M., Lawrence, J., Charles, D., Gatenby, C., Kreeger, D.A., Nightengale, T., homas R.L., Velinsky, D.J., 2002. An integrative approach towards understanding ecological responses to dam removal: the Manatawny creek study. Journal of the American Water Resources Association, 38 (6) 1581-1599.

Chapuis, M., Bright, C.J., Hufnagel, J., MacVicar, B., 2014. Detection ranges and uncertainty of passive Radio Frequency Identification (RFID) transponders for sediment tracking in gravel rivers and coastal environments. Earth Surface Processes and Landforms 39, 2109–2120.

Collins, M. J., Snyder, N. P., Boardman, G., Banks, W. S. L., Andrews, M., Baker, M. E., Conlon, M., Gellis, A., McClain, S., Miller, A., and Wilcock, P., 2017. Channel response to sediment release: insights from a paired analysis of dam removal. Earth Surf. Process. Landforms, 42: 1636– 1651.

Dépret, T., Gautier, E., Hooke, J., Grancher, D., Virmoux, V., Brunstein, D., 2017. Causes of planform stability of a low-energy meandering gravel-bed river (Cher River, France). Geomorphology 285, 58–81.

Dépret, T., Virmoux, C., Gautier, E., Piégay, H., Doncheva, M., Ghamgui, S., Mesmin, E., Saulnier Copard, S., Milleville, L., Cavero, J., Hamadouche, P., 2020. Lowland gravel-bed river recovery through former mining reaches, the key role of sand. Geomorphology, 373.

Dudill, A., Lafaye de Micheaux, H., Frey, P., Church, M., 2018. Introducing Finer Grains Into Bedload: The Transition to a New Equilibrium. J. Geophys. Res. Earth Surf., 123, 2602–2619.

Doyle, M.W., Stanley, E.H., Harbor Jon, M., 2003. Channel adjustments following two dam removals in Wisconsin. Water Resources Research, 39 (1), 1011.

East, A.E, Pess, G.R., Bountry, J.R, Magirl, C.S., Ritchie, A.C., Logana, J.B., Randlec, T.J., Mastind, M.C., Minearf, J.T., Duda, J.J., 2015. Large-scale dam removal on the Elwha River,Washington, USA: River channel and loodplain geomorphic change. Geomorphology 228, 765-786

Egan, J., Pizzuto, J.E., 2000. Geomorphic efects of the removal of the Manatawny Dam, Pottstown, PA. EOS, Transactions of the American Geophysical Union, 81 (fall meeting supplement).

Evans, J., Mackey, S.D., Gottgens, J.F., Gill, W.M., 2000. Lessons from a dam failure. The Ohio Journal of Science 100 (4), 121-131.

Evans J.E., 2007. Sediment impacts of the 1994 failure of IVEX Dam (Chagrin River, NE Ohio): A test of channel evolution models. Journal of Great Lakes Research 33 (sp2), 90-102.

Foley, M.M., Bellmore, J.R., O'Connor, J.E., Duda, J.J., East, A.E., Grant, G.E. Anderson, C.W., Bountry J.A., Collins, M.J., Connolly, P.J., Craig, L.S., Evans, J.E., Greene, S.L., Magillian, F.J., Magirl, C. S., Major, J.J., Pess, G.R., Randle, T.J., Shafroth, P.B., Torgersen, C.E., Tullos, D., Wilcox, A.C., 2017a. Dam removal: Listening in. Water Resour. Res., 53, 5229– 5246.

Foley MM, Magilligan FJ, Torgersen CE, Major JJ, Anderson CW, Connolly, P.J., Wieferich, D., Shafroth, P.B., Evans, J.E., Infante, D., Craig, L.S., 2017b. Landscape context and the biophysical response of rivers to dam removal in the United States. PLOS ONE 12(7)

Fonstad, M.A., Dietrich, J.T., Courville, B.C., Jensen, J.L., Carbonneau, P.E., 2013. Topographic structure from motion: a new development in photogrammetric measurement. Earth Surf. Process. Landforms, 38: 421-430.

Gartner, J.D, Magilligan, F.J, Renshaw, C.E., 2015**.** Predicting the type, location and magnitude of geomorphic responses to dam removal: role of hydrologic and geomorphic constraints. Geomorphology 251, 20-30.

Gilet L., Gob, F., Virmoux, C., Touche, J., Harrache, S., Gautier, E., Moës, M., Thommeret, N., Jacob-Rousseau, N., 2018. Suivi de l'évolution morphologique et sédimentaire de l'Yonne suite à la première phase du démantèlement du barrage de Pierre Glissotte (Massif du Morvan, France). Géomorphologie, relief, processus, environnement, 24 (1), 7- 29.

Gilet, L., Gob, F., Gautier, E., Houbrechts, G., Virmoux, C., Thommeret, N., 2020. Hydro-morphometric parameters controlling travel distance of pebbles and cobbles in three gravel bed streams, Geomorphology, Volume 358.

Gob F., Bravard J.-P., Petit F., 2010. The influence of sediment size, relative grain size and channel slope on initiation of sediment motion in boulder bed rivers. A lichenometric study. Earth Surface Processes and Landforms, 35, p 1535-1547.

Grant, G.E, Lewis, S.L., 2015. The Remains of the Dam: What Have We Learned from 15 Years of US Dam Removals? In Lollino, G., Giordan, D., Crosta, G., Corominas, J., Azzam, R., Wasowski, J., Sciarra, N. (Eds.): Engineering Geology for Society and Territory, 3, 31-35.

Harris, N., Evans, J.E., 2014. Channel evolution of sandy reservoir sediments following low-head damremoval, Ottawa River, northwestern Ohio, U.S.A. Open Journal of Modern Hydrology 4, 44-56.

Hart, D.D, Johnson, T.E, Bushaw-Newton, K.L., Horwitz, R.J., Bednarek, A.T, Charles, D.F, Kreeger, D.A, Velinsky, D.J, 2002, Dam Removal: Challenges and Opportunities for Ecological Research and River Restoration. BioScience, 52, 8, 669–682.

Houbrechts, G., Hallot, E., Gob, F., Mols, J., Defechereux, O., Petit, F., 2006. Frequency and extent of bed-load transport in rivers of the Ardenne. Géog. Phys. Quatern. 60 (3), 247–258.

Houbrechts, G., Levecq, Y., Peeters, A., Hallot, E., Campenhout, J.V., Denis, A.C., Petit, F., 2015. Evaluation of long-termbedload virtual velocity in gravel-bed rivers (Ardenne, Belgium). Geomorphology 251, 6–19.

Ibisate, A., Ollero A., Ballarín D., Horacio J., Mora D., Mesanza A., Ferrer-Boix C., Acín V., Granado D., et Martín-Vide J.-P., 2016. Geomorphic monitoring and response to two dam removals: rivers Urumea and Leitzaran (Basque Country, Spain). Earth Surface Processes and Landforms, 41, 2239–2255.

Jacob-Rousseau, N. and Gob, F., 2020. Le flottage du bois et ses conséquences écologiques, de l'Antiquité à l'époque contemporaine. Problèmes, matériel et méthodes pour une contribution à l'histoire environnementale. In Beau, A. and Charpentier, G., (Eds), Chantiers et matériaux de construction. De l'Antiquité à la Révolution industrielle en Orient et en Occident, 175-208.

Knighton, D.,1998. Fluvial forms and processes. A new perspective. 2nde édition, Arnold, London, 383 p.

Lejot, J., 2008. Suivi des formes fluviales par télédétection à très haute résolution. Application aux programmes de restauration de la basse vallée de l'Ain et du Haut-Rhône (Chautagne). Thèse de doctorat, Université Lumière Lyon 2, 257p.

Liébault, F., Bellot, H., Chapuis, M., Klotz, S., Deschâtres, M., 2012. Bedload tracing in a high-sediment-load mountain stream. Earth Surface Processes and Landforms, 37, 385-399.

Lisle, T.E., Cui, Y., Parker, G., Pizzuto, J.E., Dodd, A.M., 2001. The dominance of dispersion in the evolution of bed material waves in gravel-bed rivers. Earth Surface Processes and Landforms 26 (13), 1409-1420.

Magilligan, F.J., Nislow, K.H., Kynard, B.E., Hackman, A.M. 2016. Immediate changes in stream channel geomorphology, aquatic habitat, and fish assemblages following dam removal in a small upland catchment. Geomorphology 252, 158-170.

Major, J.J., O'Connor, J.E., Podolak, C.J., Keith, M.K., Grant, G.E., Spicer, K.R., Pittman, S., Bragg, H.M., Wallick, J.R, Tanner, D.Q., Rhode, A., Wilcock, P.R., 2012. Geomorphic response of the y River, Oregon, to removal of Marmot Dam. US. Geological Survey, Professional Paper 1792, 64 p.

Major, J.J., East, A.E., O'Connor, J.E., Grant, G.E., Wilcox, A.C., Magirl, C.S., Collins, M.J., Tullos, D., 2017. Geomorphic responses to dam removal in the united states - a two-decade perspective. Gravel-Bed Rivers: Processes and Disasters (13), 355-383.

Marteau, B., Gibbins, C., Vericat, D., Batalla, R.J. 2020a. Geomorphological response to system-scale river rehabilitation I: Sediment supply from a reconnected tributary. River Research and Applications, 36, 1488-1503.

Marteau, B., Gibbins, C., Vericat, D., Batalla, R.J. 2020b. Geomorphic responses to system-scale river rehabilitation II: mainstem channel adjustments following reconnection of an ephemeral tributary. River Research and Applications, 36, 1472-1487.

Miwa, H., Parker, G., 2017. Effects of sand content on initial gravel motion in gravel-bed rivers: Effects of sand content on initial gravel motion in gravel-bed rivers. Earth Surf. Process. Landforms 42, 1355–1364.

Pearson, A.J., Snyder, N.P., Collins, M.J., 2011. Rates and processes of channel response to dam removal with a sand-illed impoundment. Water Resources Research, 47 (8), W08504.

Peck, J. A., Kasper, N. R., 2013. Multiyear assessment of the sedimentological impacts of the removals of the Munroe Falls Dam on the middle Cuyahoga River, Ohio, Rev. Eng. Geol., 21, 81– 92.

Petit, F., Gob, F., Houbrechts, G., Assani, A.A., 2005. Critical unit stream power in gravel-bed rivers. Geomorphology, 69 (1-4), p. 92-101.

Pizzuto, J., 2002. Effects of dam removal on river form and process. Bioscience, 52 (8), 683-691.

Poeppl, R.E., Keesstra, S.D., Hein, T, 2017. The geomorphic legacy of small dams - An Austrian study. Anthropocene 10, 43-55.

Poux, A.S., Gob, F., Jacob-Rousseau, N., 2011. Reconstitution des débits de crues artificielles destinées au flottage du bois dans le massif du Morvan (centre de la France, 16^{e}-19^{e} siècles) d'après les documents d'archive et la géomorphologie de terrain. Géomorphologie: relief, processus, environnement, 17 (2) 143-156. DOI: 10.4000/geomorphologie.9351.

Rangel, J. M. G., Gonçalves, G. R., & Pérez, J. A.,2018. The impact of number and spatial distribution of GCPs on the positional accuracy of geospatial products derived from low-cost UASs. International Journal of Remote Sensing, 1–18

Randle, T.J., Bountry, J.A., Ritchie, A., Wille, K., 2015. Large-scale dam removal on the Elwha River, Washington, USA: Erosion of reservoir sediment. Geomorphology, 246, 709-728.

Ritchie, A.C., Warrick, J.A., East, A.E., Magirl, C.S., Stevens, A.W., Bountry, J.A., Randle, T.J., Curran, C.A., Hilldale, R.C., Duda, J.J., Gelfenbaum, G.R., Miller, I.M., Pess, G.R., Foley, M.M., McCoy, R., Ogston, A.S., 2018. Morphodynamic evolution following sediment release from the world's largest dam removal. Scientific Reports 8 (1), 13279.

Sanz-Ablanedo, E., Chandler, J.H., Rodríguez-Pérez, J.R., Ordóñez, C., 2018. Accuracy of Unmanned Aerial Vehicle (UAV) and SfM Photogrammetry Survey as a Function of the Number and Location of Ground Control Points Used. Remote Sens, 10, 1606.

Sawaske, S.R., Freyberg, D.L., 2012. A comparison of past small dam removals in highly sediment-impacted systems in the US. Geomorphology, 151, 50-58.

Schaffrath, K. R., Belmont, P., Wheaton, J. M., 2015. Landscape-scale geomorphic change detection: Quantifying spatially variable uncertainty and circumventing legacy data issues. Geomorphology, 250, 334-348.

Simons, R.K., Simons, D.B., 1991. Sediment problems associated with dam removal: Muskegon River, Michigan. Proceedings of the 1991 National Conference American Society of Civil Engineers. ASCE, New York, 680-685.

Skalak, K., Pizzuto, J., 2005. The Geomorphic Effects of Existing Dams and Historic Dam Removals in the Mid-Atlantic Region, USA. 1-12. 10.1061/40763(178)29.

Skalak, K., Pizzuto, J., Egan, J., Allmendinger, N., 2011. The geomorphic effects of existing dams and historic dam removals in the mid-Atlantic region, USA. in Sediment Dynamics Upon Dam Removal, edited by A. N. Papanicolaou and B. D. Barkdoll, Am. Soc. of Civ. Eng.

Stanley, E.H., Doyle, M.W., 2003. Trading of: the ecological effects of dam removal. Front Ecology Environment, 1 (1), 15-22.

Stewart, G.B., 2006. Patterns and Processes of Sediment Transport following Sediment-illed Dam Removal in Gravel Bed Rivers. Ph.D thesis, Oregon State University, 100 p.

Straub, T.D., 2007. Erosion dynamics of a stepwise small dam removal, Brewster Creek Dam near St. Charles, Illinois. Ph.D thesis, Colorado State University, 161 p.

Thommeret, N., Dunesme, S., Gob, F., Bilodeau, C., Tamisier V,., Virmoux, C., Brunstein, D., Kreutzenberger, K., Raufaste, S., Gilet, L., 2016. Adaptation du protocole Carhyce aux grands cours d'eau à partir de données Lidar topo-bathymétrique. Actes de la Journée Technique « Avancées, apports et perspectives de la télédétection pour la caractérisation physique des corridors fluviaux », Onema et Ministère de l'Environnement, de l'Energie et de la Mer, Nanterre, France, Mai 2016, 1-7.

Tullos, D., Wang, H. (2014). Morphological responses and sediment processes following a typhoon-induced dam failure, Dahan River, Taiwan. Earth Surface Processes and Landforms 39 (2), 245-258.

Walter, C., Tullos, D.D., 2010. Downstream channel changes after a small dam removal: using aerial photos and measurement error for context; Calapooia River, Oregon. River Research and Applications, 26, 1220-1245.

Warrick, J.A., Bountry, J.A., East, A.E., Magirl, C.S., Randle, T.J., Gelfenbauma, G., Ritchie, A.C., Pess, G.R., Leung, V., Duda, J.J., 2015. Large-scale dam removal on the Elwha River, Washington, USA: Source-to-sink sediment budget and synthesis. Geomorphology 246, 729-750.

Wilcock, P. R., Kenworthy, S.T., Crowe, J.C., 2001. Experimental study of the transport of mixed sand and gravel, Water Resources Research, 37, 3349–3358.

Wilcox, A.C., O'Connor, J.E., Major, J.J., 2014. Rapid reservoir erosion, hyperconcentrated low, and downstream deposition triggered by breaching of 38-m-tall Condit Dam, White Salmon River, Washington. Journal of Geophysical Research – Earth Surface, 119 (6), 1376-1394.

Wohl, E., Cenderelli D.A. 2000. Sediment deposition and transport patterns following a reservoir sediment release. Water Resources Research 36, 319-333.

Wolman, G. 1954. A method of sampling coarse river-bed material. Transactions of American Geophysical Union, 35 (6), 951-956.

Web references

American Rivers Dam Removal Database: https://figshare.com/articles/_/5234068

Graphical abstract